1977

Geology of the Stateline District, Utah-Nevada

Terry Moore Collins

GEOLOGY OF THE STATELINE DISTRICT, UTAH-NEVADA

BY

TERRY MOORE COLLINS, 1943-

A THESIS

Presented to the Faculty of the Graduate School of the

UNIVERSITY OF MISSOURI-ROLLA

In Partial Fulfillment of the Requirements for the Degree

MASTER OF SCIENCE IN GEOLOGY

1977

115 pages

Approved by

Sheldon Kerry Grant (Advisor) Geoa Kisvarsanyi

J. L. Rockaway

ABSTRACT

The rocks exposed in the Stateline District, Iron County, Utah and Lincoln County, Nevada, are Tertiary volcanics, which serve as hosts for gold and silver bearing quartz veins. The Miocene rhyolites and dellenites, a possible caldera, cupola-associated rock textures, and the faults and styles of deformations indicate the geologic setting of Stateline is in harmony with the tectonic framework of the southern Great Basin. Four map units, subdivided into nine members, are recognized. X-ray fluorescence analyses for SiO_2, TiO_2, Fe_2O_3, CaO, and K_2O differentiated the map units, while variations in the primary quartz, sanadine, plagioclase, biotite, hornblende, and total crystal content characterized members. Secondary minerals, determined by optical and X-ray techniques, are scarce in the second rhyolites, whereas the first rhyolites have secondary quartz and possibly clays, and the dellenite flows and lithic pumice tuff map unit have secondary calcite.

Bixbyite and associated topaz are found in the volcanic rocks of Stateline Mining District. These bixbyites have a lattice parameter of 9.415Å while reference specimens from other localities have parameters of 9.393Å to 9.428Å.

Visible alteration and high K_2O content are coincident with the distribution of veins. Gains or losses of major components, and density and porosity changes during alteration are the result of leaching, cavity filling, replacement, and recrystallization processes. Except for the pervasive recrystallization, these processes altered the rocks selectively.

Chemical variations, including high SiO_2, TiO_2, Fe_2O_3, and K_2O near one Stateline vein, are comparable with mineralogical variations adjacent to veins in a nearby fluorspar district.

TABLE OF CONTENTS

LIST OF ILLUSTRATIONS

LIST OF TABLES

I. INTRODUCTION

A. PURPOSE

A detailed study of the petrology, chemistry, and geology of the Tertiary volcanic rocks of the Stateline Mining District has not been attempted in the past. The objectives of this investigation are: to map the geology of the district, to establish the chemistry and primary mineralogy of the rock units, and to investigate the chemical patterns and secondary mineralogy of the alteration of the volcanic rocks in the district. Also, the unit cell dimensions of bixbyite, a rare mineral found near Stateline, are investigated.

B. LOCATION

The Stateline Mining District is located in Iron County, Utah and Lincoln County, Nevada. Stateline townsite is approximately 16 miles (26 km) north of Modena, Utah, at 38°N latitude and 114°W longitude. From Modena, on U. S. Highway 56, an improved dirt road leads northward up Modena Draw, toward Hamlin Valley. The Stateline District is situated on the eastern flank of the White Rock Mountains, which bound the western edge of Hamlin Valley. The study area is approximately six miles (9.7 km) by four miles (6.4 km), elongated north-south and is located in Figure 1.

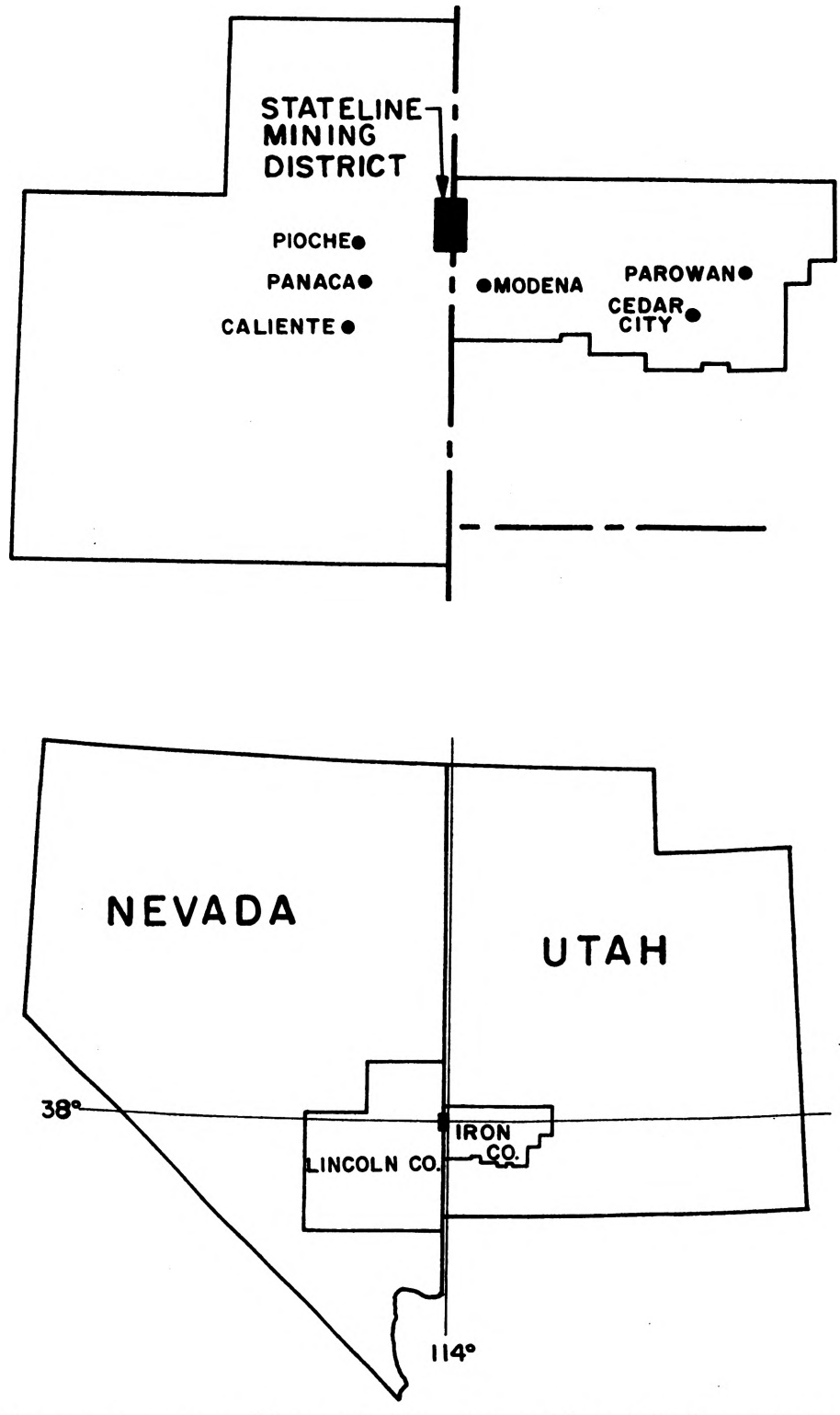

Figure 1. Location of the Stateline Mining District

C. ACKNOWLEDGEMENTS

I would like to express my gratitude to Marshall Austin for the use of his cabin in Rice Canyon and to Frank and Edna Haigh of Modena for nursing me back to health after an unfortunate accident.

I would like to thank Mrs. V. H. McNutt and the V. H. McNutt Memorial Fund for support of the field and thesis preparation expenses.

A special thanks goes to Michael R. Roberson for help in preparation of samples for laboratory study.

I am very much indebted to my advisor, Dr. S. K. Grant. He was always available with help and suggestions. His patience and understanding through the very slow evolution of this thesis was greatly appreciated.

II. PREVIOUS WORK

The first references to the Stateline District were made in two articles by Judge Grant H. Smith (1902). He noted that the range was composed of eruptive rocks of which the early flows were andesite, trachyte, tuffs, and andesitic breccia. Later came the quartz porphyry which served as host to the gold and silver bearing quartz veins. The chemistry of the rocks exposed in the Stateline Mining District cannot be correlated with the rock names used by Smith. His rock names are probably field terms. His "tuffs" are rhyolites and are the same unit as the lithic pumice tuff map unit in this thesis. Smith's andesite, trachyte, and andesitic breccia are correlated with this author's dellenite flows. The quartz porphyry of Smith is probably equivalent to the rhyolite porphyry member of the first rhyolites. Nearly all of the veins of the district were formed in a north-south fissure system, a notable exception being an east-west vein upon which the three principal mines of the district were located. The most westerly mine, the Ophir, contained principally silver ores, while the central mine, the Margaret, had ores containing equal parts of gold and silver, and the Johnny mine on the east was a gold producer. Smith included a sketch map in his publication showing the locations of the veins and producing mines.

Butler and others (1920) divided the rocks of the area into three groups that were, from oldest to youngest, rhyolite tuff, latite, and rhyolite. Alteration was extensive in the mineralized areas and consisted chiefly of replacement of the country rock by a fine grained mixture of quartz and orthoclase with minor sericite, and where alteration was slight chlorite was present. There was probably removal of soda, lime, and magnesia, and additions of potassium.

Thomson and Perry (1975) produced a reconnaissance surface map of the Stateline District and also mapped many of the underground workings, complementing them with numerous gold and silver assays.

III. REGIONAL GEOLOGY

The intrarelationships of the volcanic rocks of the Great Basin are similar to those of other volcanic fields of the west, notably the Mogollon Plateau volcanic field of southwestern New Mexico and the San Juan volcanic field of Colorado. A brief comparison of these volcanic fields might illustrate the position of rocks such as the rhyolites and dellenites of the Stateline area, in the volcanic evolution of the region. The volcanic suites that can be recognized in the Great Basin, southeastern San Juan area, and Mogollon-Datil volcanic field, and their age and stratigraphic position are illustrated in Figure 2. The rock type nomenclature used in Figure 2 is that of the authors referenced in the caption. The potassic tuffs and calc-alkalic tuffs of the Great Basin portion of Figure 2 are ash-flow tuffs. The calc-alkalic andesite to rhyolite noted in the Mogollon-Datil field contains ash-flow tuffs.

Elston and others (1976) assigned the volcanic rocks of the Mogollon-Datil field of southwestern New Mexico to three overlapping suites: calc-alkalic andesite to rhyolite (about 43-29 m. y. old), high silica alkali rhyolite (about 32-21 m. y. old), and basalt and calc-alkalic basaltic andesite (about 37-0 m. y. old).

Lipman (1975) noted that in the southeastern San Juan Mountains, during the interval 35-30 m. y. ago,

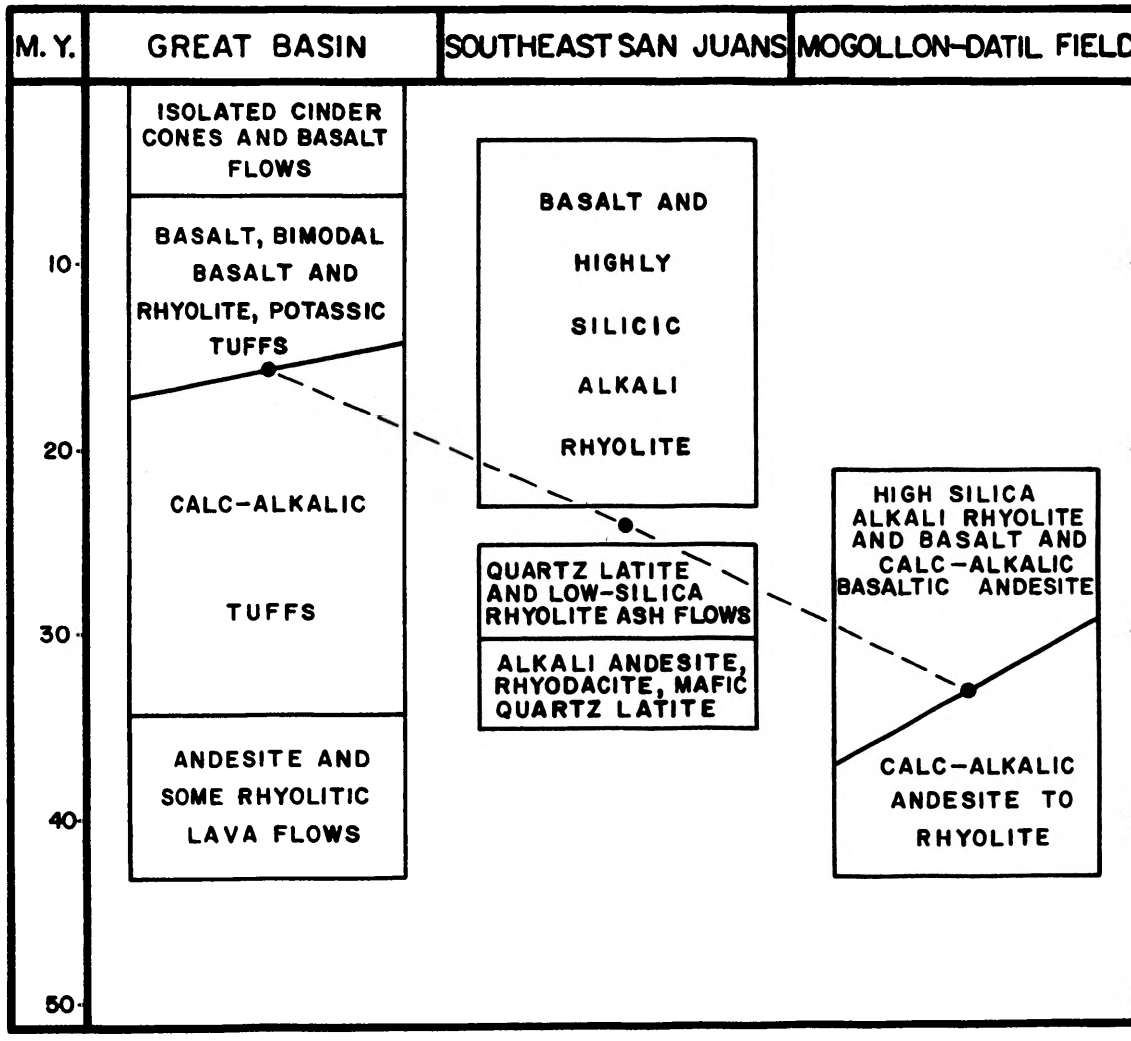

Figure 2. Stratigraphic position of the regional volcanic suites

The dashed line represents the time transition between the calc-alkalic and bimodal suites in each of the three areas. Age and nomenclature of the Great Basin rock sequence taken from Stewart and others (1977) and Noble and others (1976); southeast San Juans from Lipman (1975); and Mogollon-Datil Field from Elston and others (1976).

voluminous lavas and breccias of mainly alkali andesite, rhyodacite, and mafic quartz latite were erupted from numerous scattered central volcanoes. About 30 m. y. ago, volcanic activity changed to explosive ash-flow eruptions, associated with large calderas, of quartz latite and low silica rhyolite, that persisted until about 25 m. y. ago. During the interval 23-3 m. y. ago, volcanism again changed to a bimodal association of basalt and highly silicic alkali rhyolite.

Stewart and others (1977) recognized four groups of volcanic rocks in the Great Basin. Andesitic and some rhyolitic lava flows were widespread from 43-34 m. y. in a broad band extending from western Utah to central Nevada along latitude 40°N. The time period 34-14 m. y. ago was dominated by calc-alkalic ash-flow tuff that was concentrated in a broad, slightly arcuate east-west band at approximately latitude 38°N. The character of the volcanism during the interval 17-6 m. y. ago changed to basalt and bimodal assemblages of basalt and rhyolite. During this interval an east-trending ash-flow tuff belt (approximately latitude 37°N) extended from the Little Walker caldera of California to the Ox Valley caldera of Utah (encompassing at least eight other intervening calderas). The volcanism was described as potassic in nature by Noble and others (1976). Subsequent volcanic activity, 6-0 m. y. ago, was largely confined to isolated

cinder cones and basalt flows, mostly along the west and east borders of the Great Basin.

The general eruptive sequence that the above areas have in common is andesite followed by calc-alkalic ash flows followed by bimodal basalt and high silica alkali rhyolite.

The calc-alkalic rocks of the San Juan and Mogollon-Datil fields are believed to be differentiates of an underlying batholith. The areal distribution of the andesites and overlying ash flows are roughly the same. In contrast, the ash flows of the Great Basin are considerably south of the east-west band of andesites.

Andesite volcanism did not start at the same time in all of the areas discussed and was not of equal duration in the separate areas. The same is true for the calc-alkalic ash flows and other subsequent volcanic cycles.

Speculation as to the causes of the observed patterns involves interpretations based on plate tectonics. Atwater (1970) and Atwater and Molnar (1973) presented a model whereby subduction of the Farallon plate along a Benioff zone was responsible for the generation of calc-alkalic magmas. After collision of the Pacific and American plates approximately 30 m. y. ago, the San Andreas transform fault became active as subduction stopped. The triple point of the Pacific, American, and Juan de Fuca plates migrated northward with time to its present position near Cape Mendocino and the calc-alkalic suite volcanism

terminated in the Mogollon-Datil, San Juan, and Great Basin volcanic field at 29 m. y., 25 m. y., and 14 m. y. ago respectively. A wave of bimodal basalt and high silica alkali rhyolite volcanism swept northward following the cessation of calc-alkalic eruptions. In the Mogollon-Datil field the bimodal suite eruptions began (37-32 m. y. ago) before the end of calc-alkalic volcanism (29 m. y. ago).

Armstrong and Higgins (1973) depicted the Cenozoic basalts as being approximately 30 m. y. old in southern Arizona and southwestern New Mexico and becoming progressively younger to the northwest and northeast, over the Great Basin volcanic field and the San Juan volcanic field respectively. Christiansen and Lipman (1972) stated that the tectonic associations of most fundamentally basaltic volcanic fields probably are of extensional character. However, Elston (1976) noted that the age of Basin and Range faulting seems everywhere to be around 18 $\pm$ 3 m. y. old, yet the bimodal basalt and high silica alkali rhyolite suite of New Mexico ranges from 30-20 m. y. old, with a trickle of basaltic activity that continued until the present. Nolan (1943) concluded that Basin and Range faulting had been essentially continuous since early Oligocene time. The areal distribution of Basin and Range faulting and Cenozoic basalts are roughly the same but an age correlation between them is difficult to verify at this time.

Structures in the Stateline area may be related to those that appear regionally. The regional structures are shown in Figure 3. These include north-south normal faults, northeast and northwest strike-slip faults, and east-west lineaments and intrusive belts. The Great Basin is bounded on the southwest, northwest, and south by strike-slip faulting. The Basin and Range faulting within the Great Basin has a pronounced north-south grain that is not so well developed in other areas of the Basin and Range province. The southwestern boundary of the Great Basin can be approximated by the Walker Lane, a zone of right-lateral movement that is parallel to, and of the same movement as the San Andreas transform system. In Oregon the Basin and Range structures of the Great Basin are terminated by a northwest trending zone of right-lateral faults. Lawrence (1976) does not consider them to be a part of the San Andreas-Walker Lane right-lateral system because of a 20 degree difference in trend.

In the Lake Mead region of southern Nevada a northeast trending zone of left-lateral faults generally separates an area of Precambrian basement to the south from Paleozoic and Mesozoic sedimentary rocks on the north (Anderson and others, 1972). The southeast-trending right-lateral Las Vegas shear zone is recognized in this area but the age relationship of the two fault systems is not clear.

In addition to these strike-slip fault zones that bound portions of the Great Basin, numerous east-west

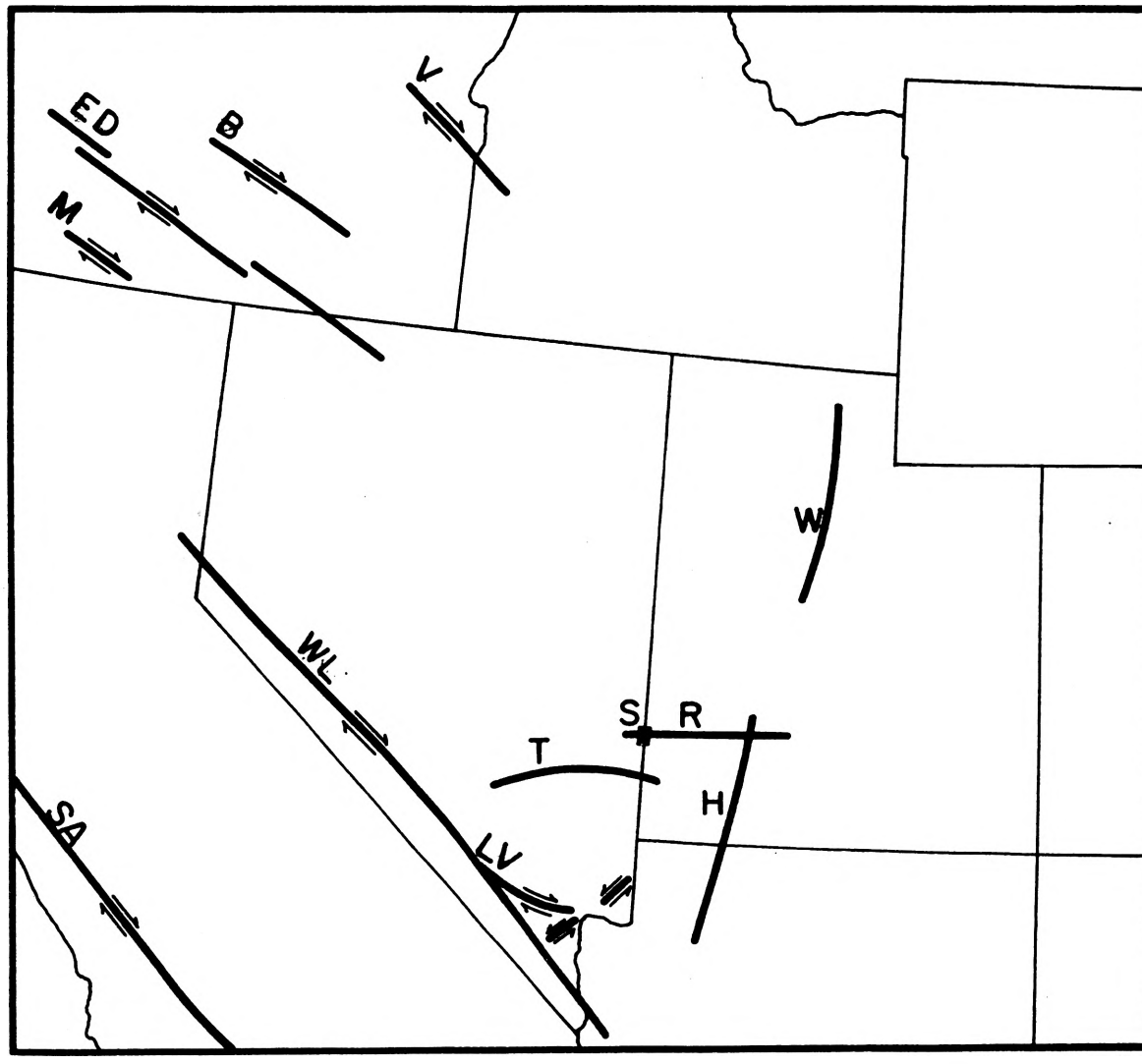

Figure 3. Regional structures of the Great Basin

W = Wasatch Fault. H = Hurricane Fault.
R = Rhyolite belt (Rowley and Anderson, 1975)
S = Stateline Mining District.
T = Timpahute Lineament. LV = Las Vegas shear zone. WL = Walker Lane. SA = San Andreas fault zone. V = Vale zone. B = Brothers fault zone. ED = Eugene-Denio zone.
M = McLaughlin zone.

lineaments have been described within the Great Basin. One such lineament in central Lincoln County, Nevada is termed by Ekren and others (1976) as the Timpahute Lineament. It is delineated by, from west to east, rhyolite and granite plugs of the Groom Range, granites of the east-west trending Timpahute Range, a zone of recent seismicity, intrusives of the Chief Range, intrusives of the Cedar Range, Caliente cauldron complex, and east-trending (probably an expression of faulting) rhyolite masses near Bull Valley, Utah.

Further north, an east-west rhyolite lineament in southern Utah has been described by Rowley and Anderson (1975).

> "Three small rhyolite plugs and domes are distributed along an east-west line through the northern Black Mountains. Two have K-Ar ages of about 10 m. y. and 7 m. y., as dated by H. H. Mehnert (unpublished data, 1975). These are part of an east-west lineament that extends at least 90 miles from the Wah Wah Mountains on the west to the Sevier Plateau on the east, and is delineated by six rhyolite plugs (Rowley and Lipman, 1975), one small caldera, hydrothermally altered rock, east-west fault trends and discontinuities in aeromagnetic anomalies. Two rhyolite plugs along the western part of the

lineament have K-Ar ages of 20 and 11 m. y. (Mehnert, unpublished data, 1975)."

An examination by the author of aerial photographs of the southern Wah Wah Range, Needle Range, southern White Rock Mountains, and Mahogany Mountains indicates that the lineament-controlled band of rhyolites described by Rowley and Anderson is continuous to the west of the Wah Wah Range for at least another 25 miles (40 km). Grant (unpublished manuscript) noted a granodiorite stock, rhyolite dikes, and east-northeast faulting in the Indian Peak fluorspar district of the Needle Range. There are rhyolite dikes and some east-west faults in the Stateline and Gold Springs mining districts of the White Rock Mountains. This lineament is 40 miles north of the Timpahute lineament. Both of these lineaments are within the rhyolite belt described by Stewart and others (1977).

The rocks of the Stateline area are similar to those in adjacent regions. The Stateline sequence, beginning with the oldest rocks, is lithic pumice tuff, dellenite flows, first rhyolites (which contain at least one lithic pumice tuff unit), and second rhyolites. The absolute age of the rhyolite sequence is not known. However, the stratigraphic position of the rhyolites can be established with a fair degree of certainty by comparison with the stratigraphic sequences of the nearby areas (Figure 4).

Approximately eight miles (13 km) north of the Stateline area, in the same range, the rhyolite sequence

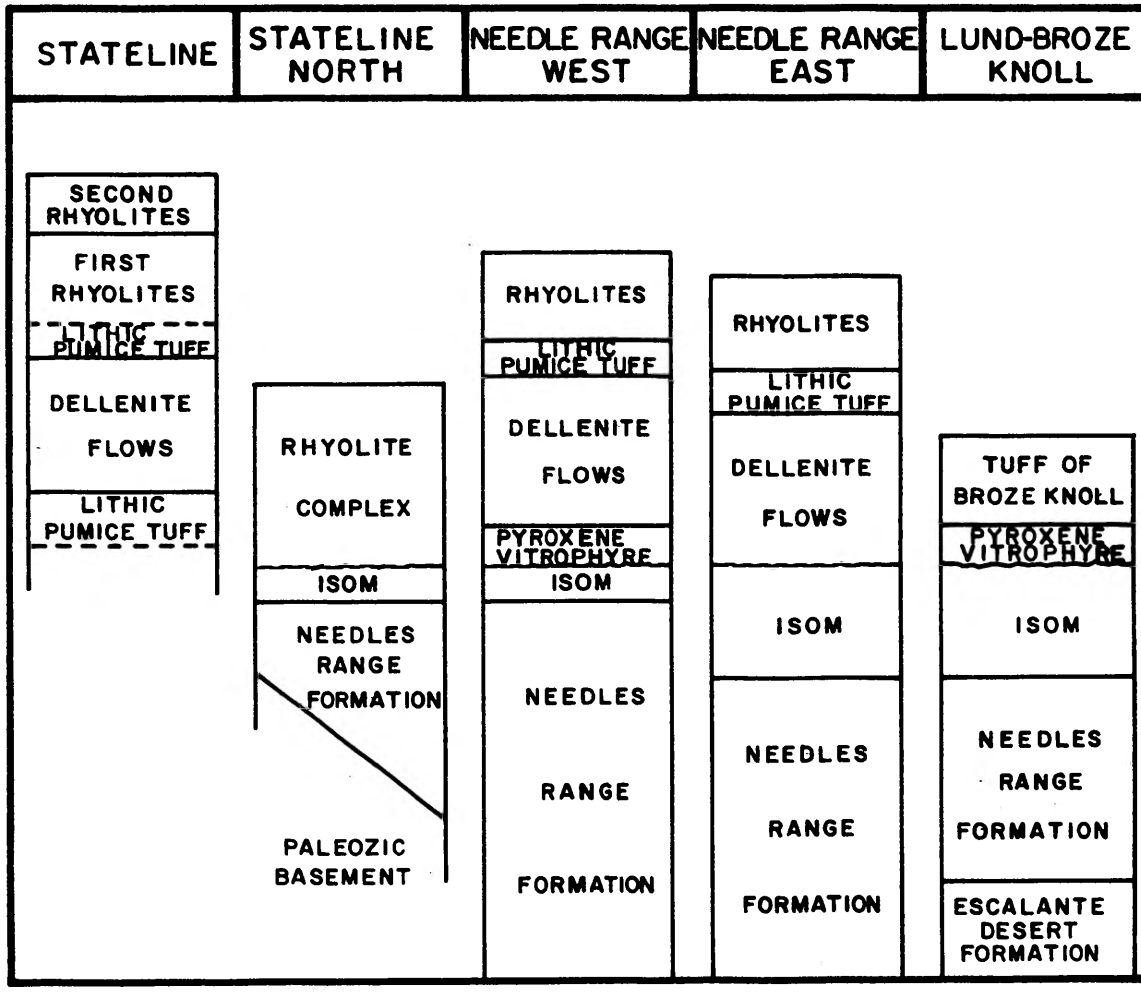

Figure 4. Stratigraphic sequences at Stateline and nearby areas

Columns for Stateline North, Needle Range East, and Lund-Broze Knoll from S. K. Grant (oral communication) and Needle Range West from J. Grossman (oral communication).

rests on the Isom Formation (25 m. y.). Near Indian Peak, on the east side of the Needle Range, approximately 15 miles (24 km) east of Stateline, a sequence of dellenite flows, a pumice tuff, and a series of rhyolites overlie, at least in part, the Isom Formation (Grant, oral communication). This sequence probably is the same as exhibited by the dellenite flows and the overlying units of the Stateline area. On the west side of the Needle Range, rocks that are probably the Isom Formation are overlain by a pyroxene-bearing vitrophyre, followed by dellenite flows, pumice tuff, and rhyolites, (John Grossman, oral communication).

Correlation of the lithic pumice tuff at the base of the Stateline section with rocks outside the Stateline area is not certain. Tuffs of similar appearance occur at several horizons in the volcanic section of the region. The oldest of these, the Escalante Desert Formation (Grant, manuscript in preparation), formerly tuffs of Escalante Valley (Best and others, 1973), near Lund, Utah, is beneath the Wah Wah member of the Needle Range Formation. The Escalante Desert Formation resembles the lithic pumice tuff at the base of the Stateline section in the field, but the chemistry of the Stateline lithic pumice tuff indicates that it is more closely related to the rhyolite sequence that is known to occur above the Isom. About 16 miles (26 km) south of Stateline, just west of Modena, Utah, is a lithic pumice tuff that resembles the

Stateline lithic pumice tuff in both chemistry and mineralogy. However, this is also an unidentified tuff of uncertain stratigraphic position. It is possible that this unidentified tuff might correlate with the tuff of Broze Knoll, (Grant, personal communication) near Lund, Utah, which rests on the Isom in places, but not enough chemical or mineralogical work has been done to make this correlation definite. There are other lithic pumice tuffs definitely within the rhyolite sequence above the Isom in southern Utah, but no attempts have been made to correlate them.

IV. ROCK TYPES

A. GENERAL STATEMENT

The mapped units were established in the field. Some of the field characteristics used to separate them were hand specimen mineralogy, size of crystals, color, presence or absence of lithophysae, presence or absence of pumice, degree of welding, and topographic expression. This proved to be satisfactory in most areas. Laterally, however, there was discontinuity of individual beds, so that the defining characteristics of each map unit were continually adjusted. In a few places, particularly where alteration had been substantial, these defining lithologic characteristics were of little value in distinguishing mapping units. A rock type that was dark in color, compact, and formed prominent outcrops would become bleached, friable, and have little or no topographic expression; a light colored porous ash-flow tuff with subdued outcrops might be silicified and stained by iron and manganese oxides, and form bold escarpments at other locations. In those areas where alteration had changed the character of the rocks so as to make it foreign in appearance, X-ray and petrographic analyses served to differentiate the map units. The lab data are discussed in a later section.

The four map units of the Stateline area, from oldest to youngest, are: the lithic pumice tuff, the dellenite

flows, the first rhyolites, and the second rhyolites. Use of the terms "first" and "second" rhyolites in this sense may imply an age relationship, the second rhyolites being younger than the first rhyolites. This age relationship is true for the bulk of the rhyolites. The terms "first" and "second" are also used here to denote petrologic types: the first rhyolites are crystal poor (up to 10 percent total crystals), flow banded, have spherulitic horizons, and exhibit thin section textures indicating that the crystals are at equilibrium with the melt from which they formed; the second rhyolites are crystal rich (up to 31 percent total crystals), glomeroporphyritic, have synneusis texture in the plagioclase, strongly embayed quartz, and graphic intergrowths between quartz and alkali feldspar. The first and second rhyolites resemble the framework and cauldron lavas respectively of Rhodes (1976), which he described in the Mogollon Plateau volcanic ring complex of New Mexico.

B. STRATIGRAPHIC RELATIONSHIPS OF MAP UNITS

The geologic map, Plate I (in pocket), has been divided into nine sectors so that areas referred to by section, township and range can be easily located. The nine sectors have been designated as northeast (NE), northcentral (NC), northwest (NW), westcentral (WC), central (C), eastcentral (EC), southeast (SE), southcentral (SC), and southwest (SW). A typical location

notation would be sec. 7, T1N, R71E, Nevada (SE), where (SE) refers to the southeast sector of Plate I. Utah and Nevada have different township and range base lines, and portions of many townships are present.

A continuous stratigraphic succession is not exposed in the mapped area, so an overall column was constructed from partial columns that are observed in widely separated localities. In sections 29 and 30, T2N, R71E, Nevada (WC), the lower portions of the column are exposed. The rocks dip westward at 15 to 45 degrees. The lithic pumice tuff is exposed on the lower gentle slopes of section 29. To the west, the steeper slopes and the first ridgeline are within the dellenite flows. Further to the west, along the prominent ridge in the south half of section 30, the first rhyolites are exposed.

The upper part of the stratigraphic column is present in sec. 29, T32S, R19W, Utah (EC). The rocks dip gently northwestward at five degrees. The low hill in the NW¼, sec. 29, is capped by second rhyolites and the southeast flank of the same hill has exposures of the first rhyolites. In the E½, sec. 6, T1N, R71E, Nevada (SW), the rocks dip 35 degrees northwestward, and the dellenite flows that are exposed at the lower elevations are overlain by the first rhyolites. The lower 50 feet of the first rhyolites, at this locality, have an included layer (vitrophyre, 10 feet or 3 meters thick) of the second rhyolite lithologic type. This indicates some intertongueing, but the

majority of the second rhyolites appear to be younger than the first rhyolites.

There is no evidence of intertongueing of the second rhyolites and first rhyolites on the east side of the district. In the NW¼, sec. 19, T32S, R19W, Utah (EC) there is a ledge-forming unit near the base of the first rhyolites. An adit driven under this ledge exposed the dellenite flows. This same ledge-former can be seen in the NE¼NW¼ sec. 24, T32S, R20W, Utah (NC). From this location to the top of Rice Mountain approximately 600 feet (183 m) of the lower first rhyolites is exposed with no second rhyolite types. Further to the south (SE), on the east side of the northeast trending Basin and Range fault, the second rhyolites are resting on the first rhyolites. Approximately 800 feet (244 m) of the upper first rhyolites is exposed in this area with no intertongueing of second rhyolite types observed. These relations suggest that the bulk of the second rhyolites are younger than the first rhyolites, at least in the eastern part of the district.

C. FIELD CHARACTERISTICS AND DISTRIBUTION OF ROCK TYPES

1. Lithic Pumice Tuff. The color of these tuffs varies from cream or sometimes pale green, through lavender to light brown. The "fresh" varieties are usually lavender in color. Crystals are sparse, and pumice lenticules and lithic fragments are abundant. The lithic fragments are light to dark gray. Two granular volcanic sandstones

approximately six inches thick are roughly 100 feet (30 m) from the top of this unit. It usually outcrops on the lower gentle slopes, but occasionally where silicified it forms prominent cliffs. The unit is probably more than 500 feet (152 m) thick.

The best exposures are in sec. 23, T32S, R20W, Utah (C) and sec. 29, T2N, R71E, Nevada (WC). Southward from this area the unit is exposed continuously for approximately two miles (3.2 km).

2. Dellenite Flows. The most obvious megascopic characteristic of the dellenite flows is the presence of abundant plagioclase and biotite phenocrysts.

The lower member of the dellenites has many varied flows of a rather dense nature and small lateral extent. The base of the lower member, where observed, is marked by a dense doreite flow (Figure 5) approximately 50 feet (15 m) thick. Overlying the doreite is a light-colored rhyolite with contorted banding that is about 30 feet (9 m) thick.

The upper member of the dellenite flows has rather uniform characteristics both vertically and laterally. The upper member has vitrophyric beds while the lower member does not.

This unit is dark red or dark gray-brown in color. Where it is altered it is decidedly lighter in color, sometimes taking on a gray-green cast. It is quite resistant to erosion, hence some of the higher peaks on

the west and north edges of the map area are dellenites. There is generally less vegetation on this unit than on the overlying rhyolites. The total thickness is probably near 1000 feet (305 m).

The best exposures of this unit are on the northern flank of Government Peak, sec. 32, T2N, R71E, Nevada (WC). The outcrop pattern of this unit is very similar to the underlying lithic pumice tuffs. It is exposed continuously to the south. It is also exposed in the southeastern part of the mapped area, in sections 1 and 6, T33S, Ranges 19W and 20W, Utah (SE).

3. First Rhyolites. The members of the first rhyolites are quite variable in appearance. Six distinct members could be recognized in the field, based on hand specimen qualities. The probable age relationships are, from oldest to youngest: lithic pumice tuff, tuff breccia, pseudosedimentary member, rhyolite porphyry, mottled member, and spheroidal member.

The lithic pumice tuff member has more pumice and fewer lithics than the lithic pumice tuff map unit. On weathered outcrops the pumice of the lithic pumice tuff member is completely destroyed, leaving disk shaped voids. In contrast, the pumice of the older lithic pumice tuff map unit appears as a lighter or darker colored lens shaped feature within the rock body. The best exposures of the lithic pumice tuff member are in the SE¼NE¼ sec. 1, T33S, R20W, Utah (SE), where it rests directly on the dellenite

flows. This member is white or cream in color and approximately 200 feet (61 m) thick.

The tuff breccia is characterized by many volcanic rock fragments (70 to 80 percent lithics). This member is pink to red in color and is probably 300 feet (91 m) thick. The only exposures are along the ridge in the SW¼NE¼ sec. 1, T33S, R20W, Utah (SC).

The pseudosedimentary member is generally white to cream in color and very porous and friable. It contains one foot thick beds of dark lithics, usually about an inch (2.54 cm) in diameter, but occasionally up to 12 inches (30 cm). There are good exposures in the SW¼ sec. 1, T33S, R20W, Utah (SC).

The rhyolite porphyry is gray to brown in color and has phenocrysts of potassium feldspars up to 8 mm in diameter and quartz up to 7 mm. The only exposures were observed along the ridgetop in the S½NW¼ sec. 31, T32S, R19W, Utah (SE).

The mottled member has a distinctive splotchy gray to red coloring and phenocrysts up to 3 mm in size. Thickness is unknown. The mottled member contains most of the veins of the district and good exposures are present near the Gold Dome mine in the SW¼ sec. 19, T32S, R19W, Utah (EC).

The spheroidal member is dark red or brown in color. Crystals are small, about one mm in size. Flow banding is prominent and in some places highly contorted.

Spherulites and/or spheroidal lithophysae are characteristic of several horizons and in some places are as large as 18 inches (46 cm) in diameter. The boundary between the mottled and spheroidal members is gradational and the combined thickness of these two members is probably in excess of 800 feet (244 m). The bulk of Rice Mountain (NE) is within the spheroidal member.

The stratigraphic relations immediately above the tuff breccia member are not clear. The tuff breccia is exposed along the ridge in the SW¼NE¼ sec. 1, T33S, R20W, Utah (SC). Northeastward along the ridge top, the tuff breccia is overlain by the rhyolite porphyry. Southwestward along the ridge in the SW¼ sec. 1, T33S, R20W, Utah (SC), the tuff breccia member is overlain by the pseudosedimentary member. There is either a fault contact at the top of the tuff breccia in one of these places or both the pseudosedimentary and rhyolite porphyry members pinch out toward the tuff breccia outcrop area.

Few samples of the tuff breccia or rhyolite porphyry were collected. Subsequent descriptions or discussions of the first rhyolites will be restricted to the lithic pumice tuff, pseudosedimentary, mottled, and spherulitic members.

4. Second Rhyolites. The base of the second rhyolites is marked by a thin ash fall tuff that is seldom exposed. Typically the exposed base of the second rhyolites is a green to black vitrophyre. It contains

spherulites, similar to those of the underlying spheroidal member of the first rhyolites, as lithics. The upper member of the second rhyolites is gray to red-brown in color and contains abundant smokey quartz, iridescent sanidine, and an occasional grain of "golden" biotite. The lower member has fewer total crystals than the upper member, and no sanidine. The low hills to the north and south of Stateline townsite are in this unit. The total thickness of second rhyolites exposed is in excess of 250 feet (76 m).

5. Dikes. Rhyolite dikes occur in the SE¼, sec. 23 and NW¼, sec. 25, T32S, R20W, Utah (C). The dikes are pale olive in color and cut the lithic pumice tuffs and spheroidal rhyolite. Small quartz veins cut the dikes.

V. STRUCTURAL CHARACTERISTICS

A. LARGE SCALE FEATURES

Figure 5 illustrates the generalized stratigraphic relationships across the Stateline area, in an east-west section. The youngest map unit of the area, the second rhyolites, was chosen as a datum and was presumed to be deposited on a horizontal surface of little relief. The first rhyolites were thicker on the east side of the district because of thickening of individual units and appearance of new members. The dellenite flows and lithic pumice tuffs were presented as being of constant thickness from west to east because limited exposures of these units on the eastern side of the district did not permit a thickness estimation to be made there.

The implication of this diagram is the presence of a basin to the east. If the dellenite flows and/or lithic pumice tuffs pinch out or thin eastward, the basin could be bounded by depositional or erosional topographic highs. On the other hand, if the dellenite flows and/or lithic pumice tuffs are of constant thickness from east to west, the basin to the east is the result of folding or faulting near the center of the mapped area.

Figure 6 is a map showing the distribution of veins in the Stateline and Gold Springs districts. The locations of the veins in the Gold Springs district were approximated from the distribution of mining claims on

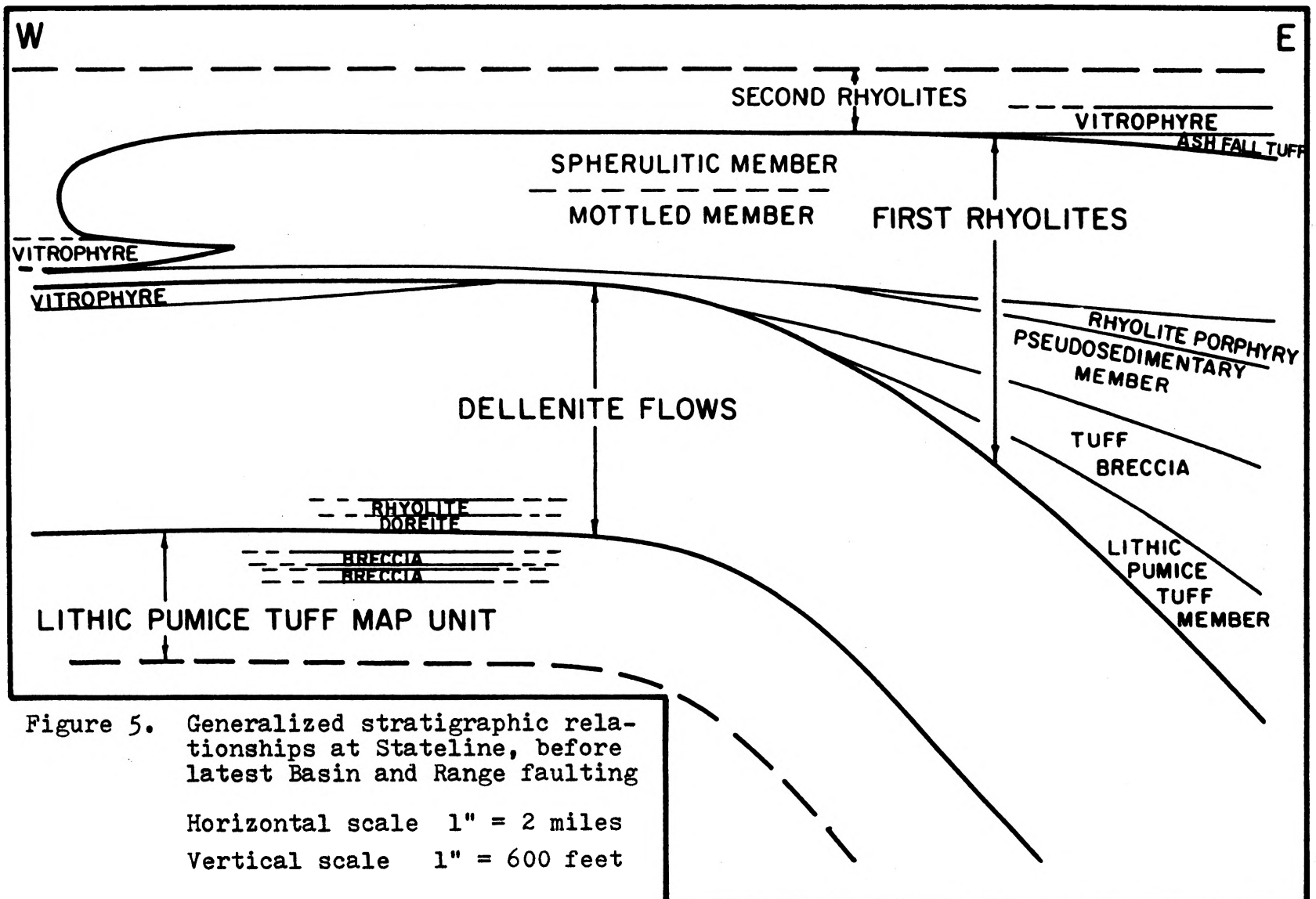

Figure 5. Generalized stratigraphic relationships at Stateline, before latest Basin and Range faulting

Horizontal scale 1" = 2 miles

Vertical scale 1" = 600 feet

Figure 6. Vein distribution of the Stateline-Gold Springs Mining Districts

Solid lines are veins. Dotted lines are veins postulated from distribution of mining claims on township plat maps. Area bounded by dashed line is part of the mapped area of Plate I. Arrows indicate the average dip direction and dip in five regions of the Stateline mapped area. Lined areas represent zones having dips in excess of 45 degrees.

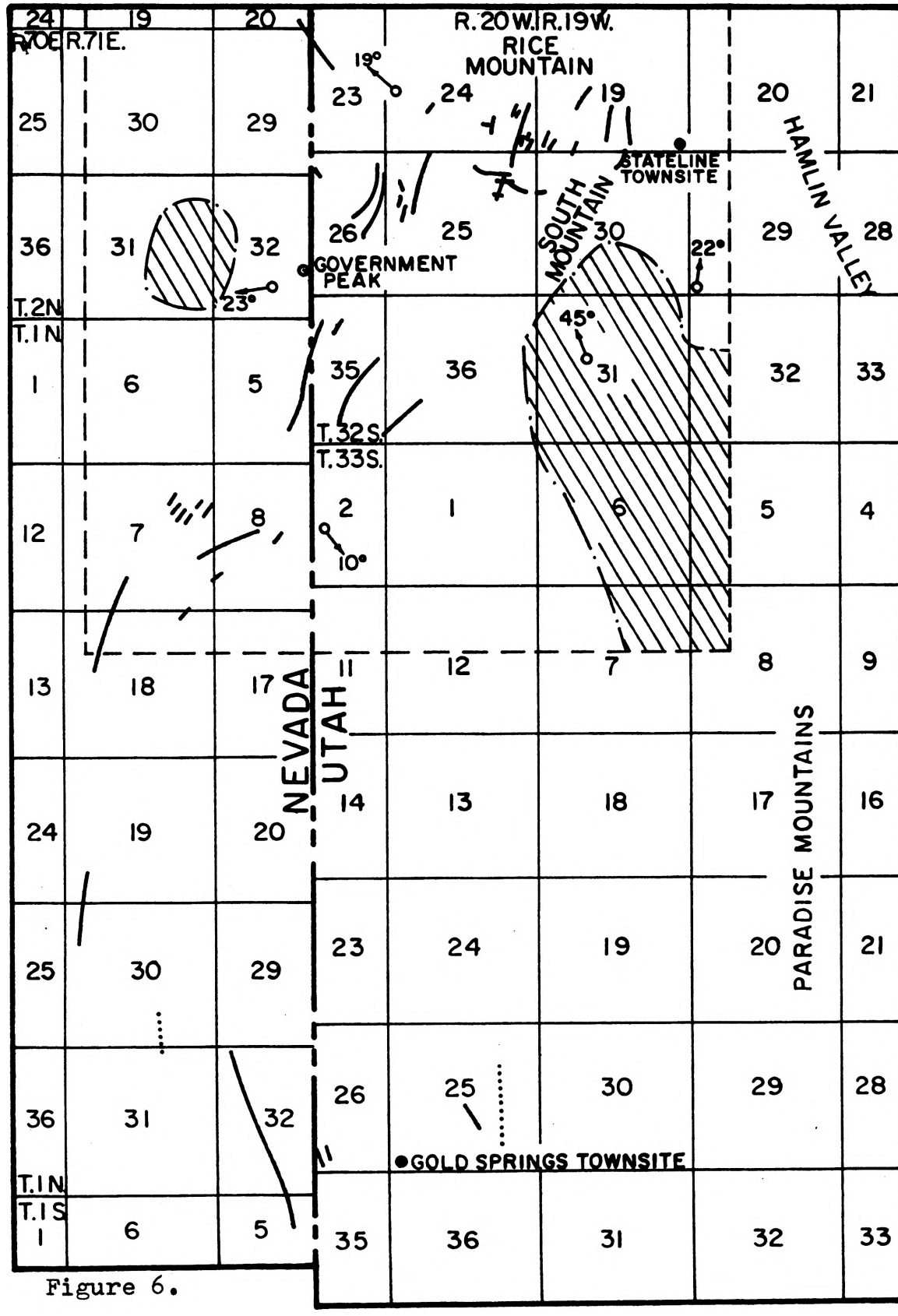
R.20W.
R.19W.
R.7E.
R.7IE.
RICE
MOUNTAIN
STATELINE
TOWNSITE
SOUTH
MOUNTAIN
HAMLIN VALLEY
GOVERNMENT
PEAK
PARADISE MOUNTAINS
NEVADA
UTAH
GOLD SPRINGS TOWNSITE
T.2N.
T.1N.
T.32S.
T.33S.
T.1N.
T.1S.
19°
23°
45°
22°
10°

Figure 6.

township plat maps or taken from Higgins (1908). The vein distribution follows a southwest trend across the mapped area of the Stateline district and then swings southeasterly through the Gold Springs townsite. The basin margin of Figure 5 coincides roughly with the vein distribution of the mapped area of the Stateline district. The veins could be associated with tension fractures along the basin edge flexure or fracture zone. Another possibility is that the arcuate distribution of the veins is associated with a collapse caldera rim. The basin assemblage of tuff breccia, rhyolites, and ash fall tuffs is characteristic of the moat areas of collapse calderas.

The lined areas of Figure 6 indicate zones which contain rocks that have dips in excess of 45 degrees. The dip directions in the larger of the hachured areas are generally to the northwest. Dips related to the basin formation would be to the southeast. Therefore, these dips are associated with some post-basin structural event, either Basin and Range faulting, caldera collapse, or flow doming.

B. ATTITUDE VARIATIONS

The rocks of the Stateline area dip northwestward at approximately 20 degrees. This figure was obtained by averaging all of the attitudes taken in the mapped area. Locally, however, dips differ radically from this figure.

Systematic attitude variations are noticed within the mapped area of Plate I. These general attitudes are

diagrammatically represented in Figure 6. The mapped area is divided into five regions, within which the attitudes are similar, but different from the other regions. The north region (NE, NC, NW, and the northern parts of EC and C) has a dip of 19 degrees to the northwest (312° azimuth). The west region (WC and parts of SW, SC, and C) has a dip of 23 degrees to the southwest (264°). The south region (parts of SW and SC) has a dip of 10 degrees to the southeast (144°). The east region (parts of SE and EC) has a dip of 22 degrees to the northeast (9°). The central region (parts of SE, C, SC, and EC) has a dip of 45 degrees to the northwest (341°). These attitudes describe a feature of radially outward dips, except for the southeast portion which has steep dips to the northwest (toward the center of the area of radial dips). Cross sections A-A' and B-B' (Plate I) also serve to illustrate the attitude variations across the Stateline area. The rocks of both cross sections have steep westward dips on the west, gentler westward dips in the central areas, and eastward dips on the east.

The majority of the attitudes that are recorded are taken from the first rhyolites. Those few attitudes that are taken from the underlying map units are consistent with those attitudes of the first rhyolites.

Two models might be advanced to explain the radial dips: one, tectonic doming, and two, volcanic doming.

Tectonic doming as used here is a deformation process that results from subsurface action, such as emplacement of a forceful intrusive. It is characterized by radial dips and radial and/or concentric fractures. Commonly graben structures are imposed upon the dome. The attitudes within graben blocks are usually compatible with the overall domal structure. Because of this, it is hard to explain the zone of steep dips in the mapped area by graben faulting.

A volcanic dome is an extrusive feature that is bulbous or mushroom shaped in cross-section. Attitudes in the center are commonly vertical. Surrounding the central area flowage features dip steeply inward. Distal portions of the volcanic dome dip away from the vent area. Underlying rocks may be uplifted or deformed by the forceful injection and extrusion of the viscous volcanic dome. Volcanic doming can explain the steep northwest dips in the southeast area.

A caldera moat area could explain the presence of 1) a basin on the east side of the mapped area that contains tuff breccia, rhyolites, and ash-fall tuffs, 2) arcuate distribution of veins from Stateline to Gold Springs, and 3) volcanic doming.

C. FAULTS

There are two major trends of faults in the Stateline area: a north-south set and an east-west set. The north-south faults, with a few exceptions, are steeply dipping

normal faults, downthrown on the east. The north-south fault that extends from (NC) through (SC) has about 1000 feet (305 m) of throw. In the NE¼ sec. 14, T32S, R20W, Utah (NC), the base of the dellenite flows is in fault contact with the first rhyolites, so that the minimum throw is the thickness of the dellenite flows, or approximately 1000 feet (305 m). The aggregate vertical separation across several faults located on Rice Mountain was calculated by projecting eastward, a cliff-forming marker horizon of the first rhyolites that is exposed in the NE¼NW¼ sec. 24, T32S, R20W, Utah (NC), to the fault located in the SE¼NW¼ sec. 19, T32S, R19W, Utah (EC). The aggregate vertical separation was calculated to be approximately 1700 feet (518 m). In the field, the marker horizon did not appear to be offset by more than 200 feet (61 m) across any individual fault, so some 900 to 1100 feet (274 to 335 m) of vertical separation in this area must be explained by hidden faults. The throw across the north-south fault that extends from (NE) through (SE) was calculated by projecting the marker bed eastward into the plane of the fault from the SE¼NW¼ sec. 19, T32S, R19W, Utah (EC), taking into account the elevation difference between the probable base of the second rhyolites adjacent to the fault and the marker bed exposure. It was also noted that there is approximately 600 feet (183 m) of first rhyolites exposed above the marker bed on Rice Mountain, and it was assumed that the top of Rice Mountain

was near the top of the first rhyolites. The minimum vertical separation across this fault is approximately 1800 feet (549 m). The true vertical separation could be considerably greater, depending upon how much of the first rhyolites has been removed from the top of Rice Mountain by erosion.

The east-west group of faults are of two types: those in which dip-slip movement is larger than strike-slip movement, and those in which strike-slip movement predominates. Both types of faults have steep dips and some of the dip-slip faults may be high angle reverse faults. The dip directions, where they can be determined, are to the north. In (NW) and the southeast corner of (WC), right-lateral faults occur. The northernmost of these has about 3000 feet (914 m) of strike-slip movement while the southernmost has about 600 feet (183 m). The movement on the strike-slip faults contrasts with that of nearby regions of the southern Great Basin, which are generally left-lateral.

VI. X-RAY CHEMISTRY OF THE VOLCANIC ROCKS

A. METHOD

Chemical analyses were determined on rock slabs by X-ray fluorescence with a General Electric XRD-5 spectrometer. The chromium tube was operated at 40 ma and 40 kvp. Helium flow rates were regulated between 0-7 SCFH, the rate depending upon the element sought. Helium pressure remained constant for each specific element. The 92 rock samples were sawed to approximately 2.5 cm by 4.5 cm by 0.5 cm slabs, so that they might later be used in the preparation of thin sections. Three determinations per element per slab were made to insure adequate time for the helium concentration in the sample chamber to come to equilibrium. Periodically a replicate slab was run to establish an instrumental drift correction.

The elements sought were silicon, titanium, iron, calcium, and potassium. The equations of Leake, et. al. (1969) were used to determine the chemical composition of the slabs. The samples and standards used to develop these equations were pressed powders of fused samples. These equations were:

$$SiO_2\ \% = 30.236x + 43.663x^2 - 42.023x^3 + 14.486x^4 - 1.756x^5 - 0.529$$

$$TiO_2\ \% = 0.768x - 0.206$$

$$Fe_2O_3\% = 10.340x - 0.193$$

$CaO \ \% = 8.218x + 0.151$

$K_2O \ \% = 0.916x + 0.029x^2 - 0.026$

where x is the count ratio of a sample to Leake's standard (BL3571). It was felt that Leake's equations could be applied to unfused powders, and also slabs, because results obtained by using his equations were similar to those based on rock powders analyzed by other laboratories. This method is a rapid one and was devised for aiding field interpretations, facilitating correlations, and spotting variations within rock bodies.

To check the reliability of the method, S. K. Grant has made intensity comparisons between powders and sawed slabs of some 77 to 100 calc-alkaline rock samples. No significant differences in intensity were noted for silicon, calcium, and potassium. However, significant systematic differences were apparent between the powders and slabs for both iron and titanium. Figures 7 and 8 show the relationships between slab and powder X-ray intensities for the elements iron and titanium respectively. Two first-order regression equations were used to describe the relationship between the slabs and powders for both iron and titanium. These equations are:

For those slabs containing less than 2.706% Fe,

$$x = 1.018x_s + 0.0135$$

For those slabs containing 2.706% Fe or more,

$$x = 2.207x_s - 0.297$$

Figure 7. Slab vs. powder response for Fe_2O_3 using paired samples

I_S = X-ray intensity from rock slab

I_P = X-ray intensity from powdered rock

I_{BL3571} = X-ray intensity from powder standard of Leake (1969)

Solid line, $I_S = I_P$

Dashed lines, least squares working curves

Data collected by S. K. Grant

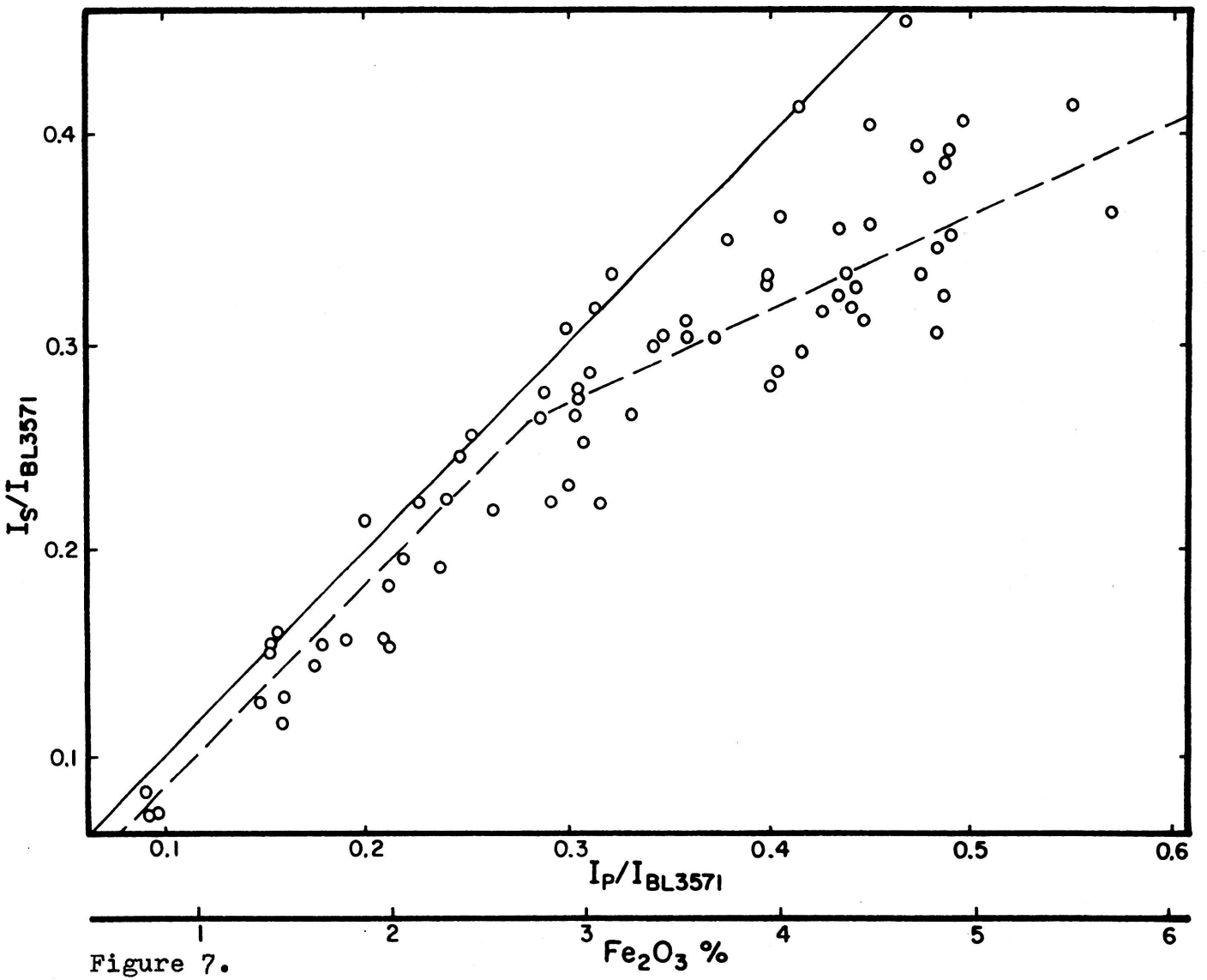

Figure 7.

Figure 8. Slab vs. powder response for TiO_2 using paired samples

I_S = X-ray intensity from rock slab

I_P = X-ray intensity from powdered rock

I_{BL3571} = X-ray intensity from powder standard of Leake (1969)

Solid line, $I_S = I_P$

Dashed lines, least squares working curves

Data collected by S. K. Grant

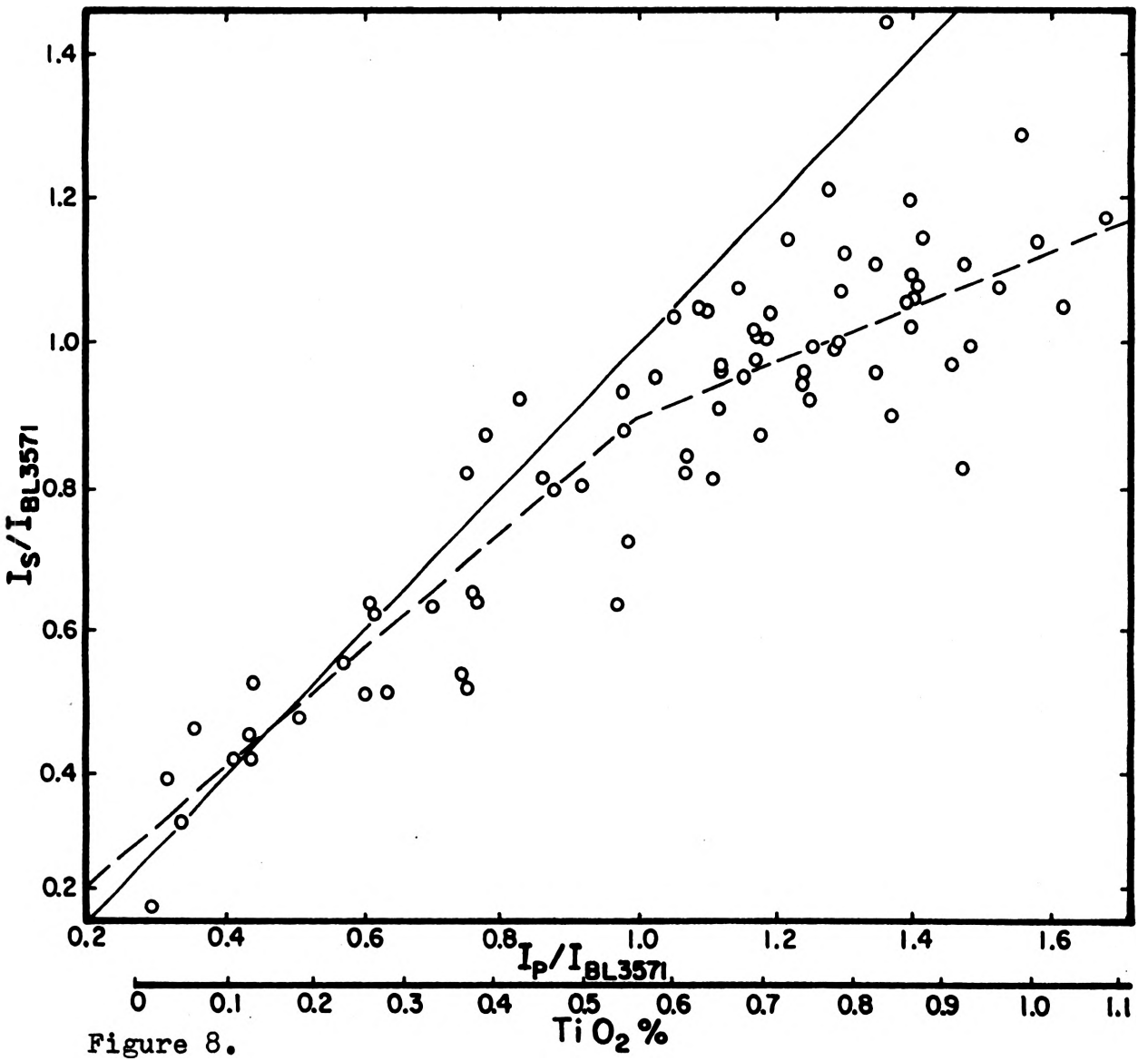
1.4
1.2
1.0
0.8
0.6
0.4
0.2
I_S/I_{BL3571}
0.2
0.4
0.6
0.8
1.0
1.2
1.4
1.6
I_P/I_{BL3571}
0
0.1
0.2
0.3
0.4
0.5
0.6
0.7
0.8
0.9
1.0
1.1
TiO_2 %

Figure 8.

For those slabs containing less than 0.565% Ti,

$$x = 1.223x_s - 0.101$$

For those slabs containing 0.565% Ti or more,

$$x = 2.636x_s - 1.369$$

where the slab correction ratio (x_s) = I_s/I_{BL3571} and (x) is the count ratio to be used in Leake's equations.

A fifth order regression equation did not reduce error significantly over the first order equations used:

	Standard Error of the estimate, ratios	Correlation Coefficient	F-test
Fe, 1st order lower curve	.100	0.882	$F_{(1,26)}$ 91.8
Fe, 1st order upper curve	.166	0.661	$F_{(1,48)}$ 37.2
Fe, 5th order	.145	0.892	$F_{(5,72)}$ 56.4
Ti, 1st order lower curve	.089	0.879	$F_{(1,23)}$ 78.2
Ti, 1st order upper curve	.143	0.440	$F_{(1,51)}$ 12.2

Analyses by atomic absorption techniques of some of the slabs and powders yielded similar results to the X-ray analyses of powders. Apparently the iron and titanium minerals, iron oxides, iron sulphides, titanium oxides, pyroxenes, and sphene, were plucked during the sawing of the slabs. Enough of the iron and titanium minerals were plucked that the X-ray analyses of the slabs were reduced, but not enough were plucked to significantly change the

atomic absorption analyses of the slabs from that of the powders. The X-ray technique is more influenced by surface properties of the slab than the atomic absorption, which employs the entire slab. Silicon, calcium, and potassium minerals were also plucked, but their percentage compositions were not radically different from the compositions of the matrix materials, so the bulk composition, as determined by X-ray techniques, was not significantly changed.

No separate individual corrections were made for background, variable grain size effects, interference by another element, rock matrix effects, or mass absorption effects because of the uncertainties in quantification of the individual factors, and because of the complexities of the calculations involved. The total effect of these factors, in so far as it differs from powders to slabs, is accounted for in the slab correction equations on pages 37 and 42.

Ten replicate analyses for oxides of each of the five major elements were determined on a single sample to establish the precision of the X-ray chemical data. These values are expressed as standard error of the mean ($s_{\bar{x}}$) in absolute percents.

Oxide	$(s_{\bar{x}})$ absolute %
SiO_2	$\pm$ 0.93
TiO_2	$\pm$ 0.029
Fe_2O_3	$\pm$ 0.033
CaO	$\pm$ 0.029
K_2O	$\pm$ 0.042

The average chemical compositions of the appropriate extrusive rocks (Nockolds, 1954) were used to name the rock types. The average percentages of SiO_2, K_2O, and CaO of each of nine extrusive rock types (calc-alkaline rhyolite, dellenite, rhyodacite, dacite, calc-alkali trachyte, latite, doreite, andesite, and tholeiitic basalt) were normalized to 100% and a ternary diagram SiO_2 - K_2O - CaO was constructed to show the compositional field of each rock type. These field boundaries were constructed by extending the perpendicular bisector of a line connecting the average normalized composition of a rock type with that of an adjacent average normalized rock type composition, until it intersected an adjacent perpendicular bisector. The compositional fields thus defined are bounded by the perpendicular bisectors and/or the edge of the diagram.

The calc-alkali suite of standard and sample averages for SiO_2 (normalized) are all above 80%. Thus, the ternary system diagram represents the area 80-100% SiO_2, 0-20% K_2O, and 0-20% CaO as depicted in Figure 9.

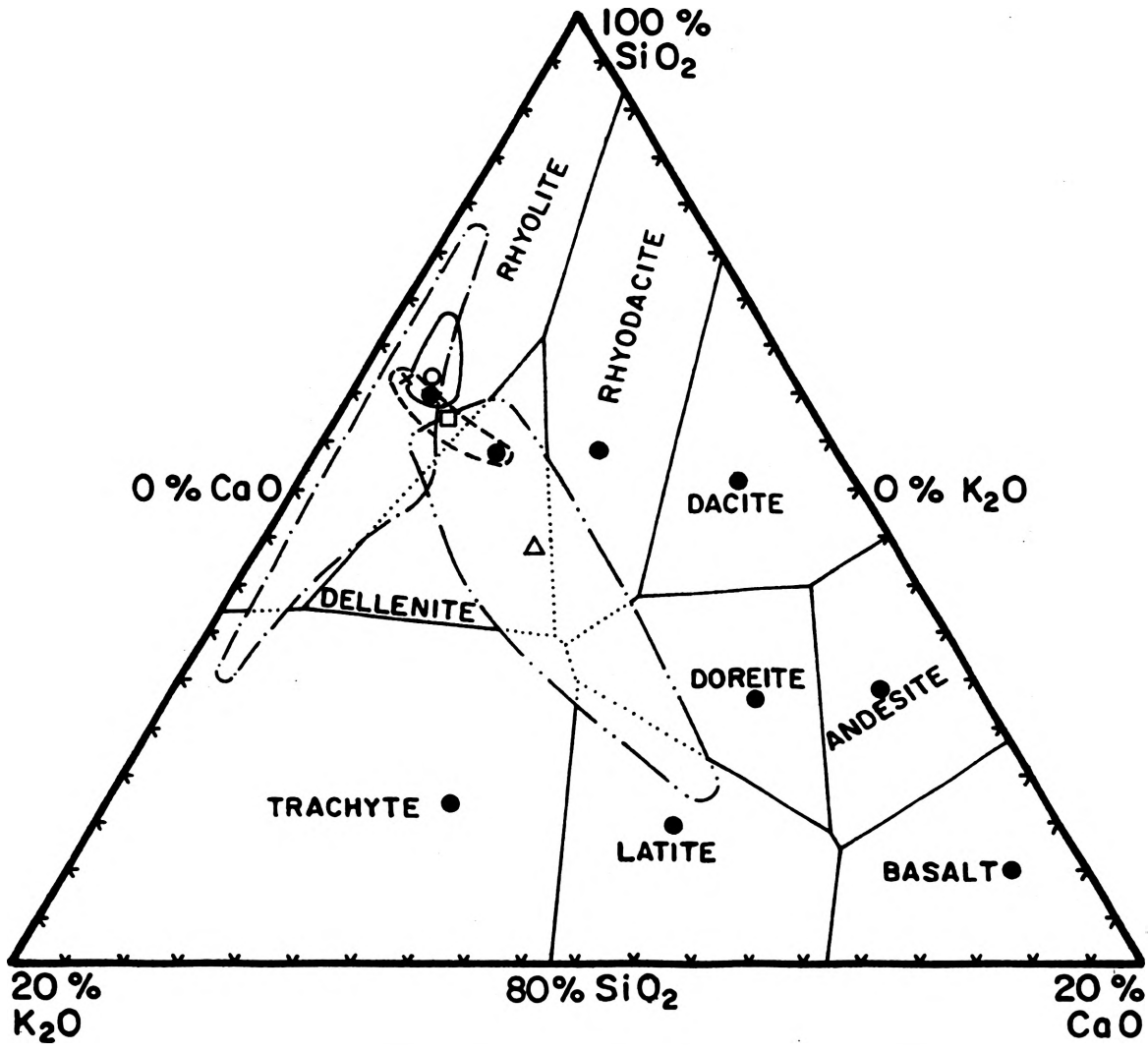

Figure 9. General composition fields for the map units

Normalized (see text) compositions are used.
Rock type averages denoted by solid circles.

	Mean Composition	Field Boundary
second rhyolites	o	———
first rhyolites	×	——·——·
dellenite flows	△	——··——
lithic pumice tuff	□	- - - - - -

The normalized composition for the nine rock types used to establish the reference fields are:

	SiO_2	K_2O	CaO
calc-alkali rhyolite	91.91	6.68	1.41
dellenite	91.34	5.86	2.80
rhyodacite	90.83	4.13	5.04
dacite	90.17	1.99	7.84
calc-alkali trachyte	83.37	10.55	6.08
latite	82.84	6.79	10.37
doreite	85.54	3.97	10.49
andesite	85.72	1.75	12.53
tholeiitic basalt	81.89	1.32	16.79

The normalized individual samples were compared to the reference fields to determine rock names.

B. RESULTS

The means ($\bar{x}$) and standard errors of the means ($s_{\bar{x}}$) of the various members and map units are tabulated in Table I. The composition of the dellenite flows is considerably different than that of the other map units. The dellenite flows have more CaO, TiO_2, and Fe_2O_3 and less SiO_2 and K_2O than the various rhyolites. The first rhyolites appear to be lower in CaO and higher in SiO_2 and K_2O than the lithic pumice tuff or second rhyolites. These differences express themselves across whole map units and are primary chemical differences among the map

TABLE I

GROUPED CHEMICAL COMPOSITIONS

Means

	SiO_2 %	TiO_2 %	Fe_2O_3* %	CaO %	K_2O %
Second Rhyolites	76.19	0.02	0.95	1.03	5.28
upper member	76.57	0	0.85	1.01	5.26
lower member	76.00	0.03	1.00	1.05	5.28
First Rhyolites	79.47	0.03	1.13	0.62	5.96
spheroidal member	78.91	0.02	1.08	0.62	6.11
mottled member	79.97	0.05	1.19	0.74	6.93
pseudosedimentary member	83.29	0.01	1.34	0.44	4.39
lithic pumice tuff member	76.63	0.05	0.96	0.58	5.44
Dellenite Flows	67.05	0.88	3.93	3.71	4.79
upper member	66.32	0.80	3.99	3.92	4.64
lower member	67.88	0.96	3.86	3.47	4.95
Lithic Pumice Tuff	77.00	0.12	1.17	1.74	5.46

Standard Errors of the Means

Second Rhyolites	1.31	0.02	0.12	0.11	0.20
upper member	1.27	0	0.17	0.12	0.47
lower member	1.86	0.03	0.16	0.16	0.17
First Rhyolites	0.77	0.007	0.06	0.04	0.25
spheroidal member	1.17	0.007	0.11	0.03	0.35
mottled member	1.90	0.01	0.07	0.14	0.69
pseudosedimentary member	1.80	0.01	0.06	0.02	0.17
lithic pumice tuff member	0.93	0.03	0.18	0.06	0.55
Dellenite Flows	0.83	0.09	0.32	0.43	0.17
upper member	1.10	0.09	0.38	0.77	0.17
lower member	1.27	0.17	0.54	0.32	0.29
Lithic Pumice Tuff	0.97	0.04	0.11	0.56	0.23

* total iron, expressed as Fe_2O_3

units. Members within map units cannot be distinguished by chemistry alone.

The major element compositions, as determined by rapid analysis techniques, of the 92 rock slabs are compiled in Table II. The slabs are divided into map units and further subdivided into members of map units. This categorization is based on field relations and thin section mineralogy, as well as chemical analyses.

Each sample number is preceeded by H (high degree of alteration) or L (low degree of alteration) as determined in thin section. These groups will be discussed in the chapter devoted to alteration.

The pre-alteration rock type for each of the map units is placed in parentheses following the map unit name. The map unit means of Table I are compared, by inspection, with the standard rock compositions of Nockolds (1954) to determine these pre-alteration rock names. SiO_2, TiO_2, and Fe_2O_3 are given more weight in this comparison because the TiO_2 and Fe_2O_3 are relatively immobile during alteration and because SiO_2 can change considerably without affecting the rock name.

Each sample number in Table II is followed by a rock type name that is derived by comparing the normalized percents SiO_2, CaO, and K_2O of the sample to that of the standards of Nockolds, as presented in Figure 9.

TABLE II

SAMPLE COMPOSITIONS AND APPARENT ROCK TYPES

Unit and rock name	Sample Number	SiO_2 %	TiO_2 %	Fe_2O_3 %	CaO %	K_2O %	apparent rock name of each sample
Second Rhyolites (rhyolite)							
upper member	L*72C35	77.84	0	0.67	1.13	5.73	rhyolite
	H*73C81	75.29	0	1.03	0.88	4.79	rhyolite
lower member	L 72C32	76.78	0.13	1.46	1.46	5.43	rhyolite
	L 73C77	71.65	0	0.86	1.11	5.28	rhyolite
	L 73C78	74.98	0	0.88	0.80	5.62	rhyolite
	H 73C80	80.59	0	0.78	0.82	4.80	rhyolite
First Rhyolites (rhyolite)							
spheroidal member	L 72C18	78.67	0.06	1.81	0.61	5.46	rhyolite
	L 72C24	83.53	0.03	1.67	0.50	5.44	rhyolite
	H 72C26	71.56	0	1.06	0.54	5.36	rhyolite
	L 72C29	82.82	0.01	1.13	0.61	6.38	rhyolite
	H 72C31	80.54	0.10	1.24	0.54	9.60	rhyolite
	H 72C33	82.56	0.06	2.37	0.71	6.13	rhyolite
	H 72C43	86.38	0	0.73	0.42	9.21	rhyolite
	L 72C45	82.50	0	0.39	0.44	8.14	rhyolite
	H 72C47	72.95	0	0.37	0.62	6.20	rhyolite
	L 72C49	83.01	0	0.91	0.85	5.67	rhyolite
	L 72C50	84.12	0	0.50	0.48	5.30	rhyolite
	L 72C52	74.65	0	1.05	0.76	5.76	rhyolite
	H 72C53	81.29	0	1.07	0.66	5.11	rhyolite
	H 72C56	76.98	0	1.12	0.60	5.14	rhyolite
	L 72C68	69.21	0	0.99	0.77	4.11	rhyolite
	H 72C69	72.37	0	1.07	0.73	4.25	rhyolite
	L 72C72	83.21	0	0.88	0.39	7.81	rhyolite

Table II. (continued)

Unit and rock name	Sample Number	SiO_2 %	TiO_2 %	Fe_2O_3 %	CaO %	K_2O %	apparent rock name of each sample
	L 72C75	73.23	0	1.01	0.69	4.71	rhyolite
	H 73C97	79.62	0.05	1.17	0.79	6.35	rhyolite
mottled member	L 72C28	70.96	0.09	1.31	0.96	6.24	rhyolite
	L 72C30	89.95	0.07	1.09	0.61	4.43	rhyolite
	H 72C34	84.74	0	1.32	0.84	6.32	rhyolite
	H 72C62	78.79	0.10	1.35	0.47	9.90	rhyolite
	H 72C63	80.39	0.07	1.12	0.47	7.07	rhyolite
	L 72C64	80.75	0	1.16	0.55	4.95	rhyolite
	H 72C65	76.45	0.04	1.02	1.97	6.64	dellenite
	L 72C66	86.91	0.01	0.78	0.50	4.78	rhyolite
	L 72C71	72.40	0.06	1.60	0.57	11.03	trachyte
	L 73C99	78.36	0.06	1.11	0.50	7.97	rhyolite
pseudosedimentary member	H 72C42	76.21	0	1.29	0.47	4.42	rhyolite
	L 72C46	80.72	0.08	1.30	0.42	4.67	rhyolite
	L 72C58	83.60	0	1.42	0.45	4.52	rhyolite
	H 72C59	88.86	0	1.20	0.36	4.47	rhyolite
	H 72C60	84.19	0	1.27	0.46	4.70	rhyolite
	L 73C98	86.17	0	1.58	0.47	3.57	rhyolite
lithic pumice tuff member	H 72C14	74.72	0.14	0.93	0.53	7.10	rhyolite
	H 72C48	76.96	0	0.28	0.35	6.84	rhyolite
	H 73C83	80.46	0	0.81	0.60	5.00	rhyolite
	L 73C85	74.49	0.15	1.64	0.65	5.34	rhyolite
	L 73C87	77.84	0	1.10	0.81	4.92	rhyolite
	L 73C89	75.31	0	0.98	0.56	3.45	rhyolite

Table II. (continued)

Unit and rock name	Sample Number	SiO_2 %	TiO_2 %	Fe_2O_3 %	CaO %	K_2O %	apparent rock name of each sample
Dellenite Flows (dellenite)							
upper member	L 72C02	62.86	1.03	3.43	6.20	4.20	doreite
	L 72C04	67.14	0.99	4.31	3.17	4.71	dellenite
	L 72C05	62.51	0.52	2.37	2.27	4.43	dellenite
	H 72C19	69.65	0.71	4.25	8.98	4.79	latite
	H 72C36	66.87	1.22	4.65	3.17	5.84	dellenite
	H 73C76	63.64	0.74	4.48	2.03	4.08	dellenite
	H 73C91	63.68	0.94	6.05	4.10	4.79	dellenite
	L 73C95	71.67	0.39	2.47	2.04	4.38	dellenite
	L 73C96	68.84	0.64	3.88	3.33	4.50	dellenite
lower member	H 72C12	65.64	1.07	3.93	2.45	5.54	dellenite
	L 72C15	67.48	0.75	2.77	3.04	5.48	dellenite
	L 72C16	68.97	1.21	5.61	3.29	4.85	dellenite
	L 72C22	62.31	1.40	4.61	4.58	3.88	rhyodacite
	L 72C54	73.01	0.21	1.57	2.34	4.31	dellenite
	L 72C57	72.12	0.54	2.93	3.28	6.37	dellenite
	L 73C92	68.46	0.87	3.33	4.03	4.17	rhyodacite
	H 73C93	65.07	1.66	6.10	4.74	5.02	rhyodacite
Lithic Pumice Tuff (rhyolite)							
	L 72C17	79.47	0.21	1.24	0.68	5.98	rhyolite
	H 72C20	74.75	0.04	0.89	2.28	5.27	dellenite
	L 72C21	76.83	0.15	1.14	0.94	5.69	rhyolite
	H 72C51	76.93	0.07	1.42	3.05	4.90	dellenite
Altered slabs, sediments, and ash-fall tuffs							
	72C01	75.48	0.32	1.41	0.79	4.78	rhyolite
	72C03	70.25	0.11	1.14	2.06	5.85	dellenite

Table II. (continued)

Unit and rock name	Sample Number	SiO_2 %	TiO_2 %	Fe_2O_3 %	CaO %	K_2O %	apparent rock name of each sample
	72C06	85.29	0	0.60	0.75	5.69	rhyolite
	72C07	75.62	0.02	0.77	1.08	4.92	rhyolite
	72C08	71.41	0.09	1.08	2.05	6.38	dellenite
	72C09	69.51	0.36	1.91	1.29	7.15	rhyolite
	72C10	78.75	0	0.59	0.83	5.20	rhyolite
	72C13	61.70	1.94	9.31	4.76	3.11	rhyodacite
	72C23	71.64	1.36	6.80	1.79	2.61	rhyolite
	72C25	64.08	0	1.01	0.59	5.88	rhyolite
	72C27	66.14	0.87	4.90	3.26	3.96	dellenite
	72C44	70.78	0.87	7.97	0.76	5.34	rhyolite
	72C55	75.09	0	1.03	2.29	3.34	dellenite
	72C67	73.44	2.67	1.43	0.36	0.18	sediment
	72C70	59.62	0	1.11	1.71	2.68	dellenite
	72C73	72.30	0	1.04	0.92	5.81	rhyolite
	72C74	73.44	0	0.60	2.18	3.47	dellenite
	73C79	72.82	0	0.81	2.39	3.70	dellenite
	73C82	72.07	0.23	2.37	1.32	5.64	rhyolite
	73C84	78.31	0	1.33	1.94	5.61	rhyolite
	73C86	74.15	0	1.42	1.98	4.46	dellenite
	73C88	74.32	0.09	1.42	2.14	3.90	dellenite
	73C90	84.13	0	0.51	0.44	11.32	rhyolite
	73C94	72.90	0.19	1.16	1.31	6.62	rhyolite

* L and H denote low and high alteration groups

Any rock naming problems that become apparent at the time of the normalizing procedure can be solved by checking the raw oxide percents against Nockolds' averages. Rock names different from the original rock names could be caused by chemical changes in the key oxides during alteration. The oxides that are typical of the original rock type are accepted. Those that differ from the original type are suspect. The original rock type of the first rhyolites is a rhyolite. Sample 72C65 of the mottled member of the first rhyolites has enough CaO to be named a "dellenite," even though the remainder of the oxides indicate it is a rhyolite. This suggests that part of the CaO was introduced by some secondary process, probably hydrothermal alteration. Sample 72C71, a "trachyte," in the mottled member of the first rhyolites, has K_2O added and SiO_2 subtracted. Samples 72C02, a "doreite," and 72C19, a "latite," both in the upper member of the dellenite flows, have CaO added. Samples 72C22, 73C92, and 73C93, "rhyodacites," in the lower member of the dellenite flows, have CaO added. Samples 72C20 and 72C51, "dellenites" of the lithic pumice tuff, have CaO added. All of the questionable rock type names listed above, except one, are caused by CaO additions. Sample 72C71 with a K_2O addition and SiO_2 subtraction, is from the horizon that serves as host for most of the veins of the district.

Hypothetically, the proportions of the three key oxides could be consistent with a rock name, but their absolute value might be far from Nockolds' average. For example, a rock that is 8% SiO_2, 0.1% CaO, and 0.5% K_2O would have the same normalized composition as a rock that is 80% SiO_2, 1% CaO, and 5% K_2O. This situation is obvious when the raw oxide percents are checked. However, this event did not occur in this investigation.

VII. MINERALOGY OF THE VOLCANIC ROCKS

A. PRIMARY MINERALOGY

Thin sections were made of each of the 92 rock slabs. The thin sections were studied with an Olympus polarizing optical microscope. A grid ocular and stage micrometer were used to determine the percents of quartz, sanidine, plagioclase, biotite, hornblende, and total crystals. The mineralogy of the thin sections is tabulated in Appendix A.

The mean crystal percent and standard error of the means of the various members and map units are included in Table III. The map units have different crystal percents. The second rhyolites are crystal rich and quartz rich; the first rhyolites are crystal poor with significant sanidine; the dellenite flows are crystal rich, high in plagioclase and biotite; the lithic pumice tuff unit is crystal poor with significant biotite. The second rhyolites could be confused with the dellenite flows on the basis of mean total crystal percent, but not when individual mineral percents are considered. The second rhyolites have ten times the quartz of the dellenite flows. The dellenite flows have no sanidine, but the upper member of the second rhyolites has 12.92 percent sanidine. The second rhyolites have half as much plagioclase as the dellenite flows. Biotite is high (5.02 percent) in the dellenite flows and very low in the

TABLE III

GROUPED MINERALOGICAL COMPOSITION, PHENOCRYSTS

	Means					
	Quartz	Sanidine	Plagioclase	Biotite	Hornblende	Total Crystals
	%	%	%	%	%	%
Second Rhyolites	8.61	4.31	10.81	0.28	0.13	24.14
upper member	9.34	12.92	9.17	0	0	31.42
lower member	8.25	0	11.63	0.43	0.20	20.51
First Rhyolites	3.59	3.52	0.95	0.11	0.006	8.18
spheroidal member	3.59	2.77	0.81	0.14	0	7.31
mottled member	3.49	4.20	1.28	0.16	0.03	9.18
pseudosedimentary member	4.64	5.14	0.14	0.04	0	9.96
lithic pumice tuff member	2.43	2.67	1.60	0	0	6.70
Dellenite Flows	0.82	0	19.65	5.02	0.45	25.94
upper member	1.54	0	21.04	6.13	0.68	29.39
lower member	0.02	0	18.09	3.77	0.19	22.06
Lithic Pumice Tuff	2.59	0.86	2.27	0.46	0	6.18
	Standard Error of the Means					
Second Rhyolites	2.56	0.64	1.42	0.14	0.14	2.95
upper member	7.33	1.91	1.33	0	0	6.75
lower member	1.15	0	2.03	0.20	0.21	2.86
First Rhyolites	0.35	0.50	0.27	0.04	0.007	0.63
spheroidal member	0.63	0.68	0.28	0.08	0	0.68
mottled member	0.63	0.95	0.73	0.08	0.02	1.45
pseudosedimentary member	0.25	1.71	0.14	0.04	0	1.73
lithic pumice tuff member	0.92	1.16	1.13	0	0	2.20
Dellenite Flows	0.30	0	0.97	0.55	0.19	0.97
upper member	0.56	0	1.23	0.46	0.33	1.48
lower member	0.02	0	1.52	1.05	0.17	1.22
Lithic Pumice Tuff	0.94	0.47	0.93	0.14	0	1.35

second rhyolites.

The lithic pumice tuff cannot be differentiated from the first rhyolites by total crystals. The lithic pumice tuff map unit has pumice lenticles while the first rhyolites do not, with the exception of the lithic pumice tuff member. The lithic pumice tuff member of the first rhyolites has no biotite while the lithic pumice tuff map unit has 0.46 percent biotite.

The upper member of the second rhyolites has 12.92 percent sanidine and 31.42 percent total crystals while the lower member of the second rhyolites has no sanidine and only 20.51 percent total crystals.

To check the validity of the point counts, an ANOVA model was devised to test the significance of those counts in thin sections, members, and map units by comparing mean squares of each to that of the traverses. Each point count traverse is an average of from 20 to 25 closely spaced fields of nine points each; a thin section represents two or three traverses; there are from two to eighteen thin sections per member; and from one to four members per map unit.

The significant values of the ANOVA model indicate those minerals that are important as a classification tool in any particular category. In the among-map-units category the significant F value for quartz indicates that at least one of the four map units has an unique quartz content. An inspection of the quartz means of

Table III indicates that the second rhyolites and dellenite flows have quartz percents distinctively different from the overall mean. The first rhyolites and lithic pumice tuff map units have similar quartz values but can be distinguished by sanidine percents. In the among-members, within-map-units category, quartz, plagioclase, and hornblende percents are relatively uniform. The members may be separated on the basis of sanidine, biotite, and total crystal percents. In the among-thin-sections, within-members category the significant minerals probably indicate that the members are made up of many flows, and these flows were of relatively uniform plagioclase and biotite content.

Any significant value in the ANOVA model may be due to one or more of the component items that contribute to that F. An inspection of the means of Table III and the individual percents of Appendix A indicates that the significant values of Table IV are caused by about one-half of the components. A single mean is responsible for the significance in only rare cases where the overall significance is marginal, such as in some minerals of the among-thin-sections category.

B. GROUNDMASS AND SECONDARY MINERALS

The mineralogy of the groundmass and secondary minerals on phenocrysts were determined for each sample. Microscope methods on thin sections and whole rock X-ray diffraction of unpowdered slabs were employed.

TABLE IV

ANALYSIS OF VARIANCE, MINERALOGICAL COMPOSITION

	Quartz	Sanidine	Plagioclase	Biotite	Hornblende	Total Crystals
among map units						
$F_{(3,98)}$	42.51*	43.24	234.58	106.20	7.35	174.21
variance	7.688	0.453	112.385	7.657	0.045	113.11
among members, within map units						
$F_{(5,98)}$	2.27	39.15	1.84	5.53	2.23	10.90
variance	0.039	7.634	0.607	0.576	0.008	12.191
among thin sections, within members						
$F_{(57,98)}$	2.16	3.53	1.19	1.61	1.77	1.80
variance	3.068	3.858	1.293	0.638	0.093	7.637
among traverses, within thin sections						
variance	6.522	3.781	16.483	2.596	0.299	23.642

* underlined F's are significant at the 1% level

Minerals identified by microscope methods are designated by an identifying abbreviation on the right side of Table V. The minerals identified by X-ray diffraction are depicted by a number in the main body of the table, under the appropriate mineral column. This number indicates the number of samples in which the mineral appeared. Each map unit is divided into a high alteration group and a low alteration group and further subdivided into members.

Adjacent to veins, where the secondary minerals were obviously hydrothermal, the grain size ranged up to two or three mm, sometimes exceeding the grain size of the primary minerals. The grain size of the secondary minerals in the majority of the samples ranged from 10^{-1} cm to 10^{-6} cm, with 10^{-3} cm as the lower range of microscope identification. X-ray diffraction techniques work below 10^{-3} cm. Peak broadening, which occurs near 10^{-5} cm grain size, was observed only in the clay minerals, so the majority of the secondary minerals in all samples were in the 10^{-3} cm to 10^{-5} cm size range.

The samples of the second rhyolites were all relatively fresh when compared to the other map units. The second rhyolites were divided into high and low alteration groups even though the alteration intensity index number of each of the samples was less than three on a scale of one to five. No secondary minerals were identified by microscope techniques. Only feldspars could be recognized in the low

TABLE V

MINERALOGY OF THE GROUNDMASS AND SECONDARY MINERALS

K - K feldspar	Ox- opaque oxides	S - sericite	Bx- bixbyite
Cl- chlorite	C - calcite	B - biotite	Hm- hematite
Q - quartz	Ab- albite	T - topaz	

			X-RAY IDENTIFICATION				OPTICAL IDENTIFICATION OF SECONDARY MINERALS
	Number of Samples	Alteration Group	Zeolites	Quartz	K feldspar	Plagioclase	clays**
Second Rhyolites							
upper member	1	H		1	1	1	*T,Bx,Hm
	1	L		1		1	
lower member	1	H		1	1	1	
	3	L			1	1	
First Rhyolites							
spheroidal member	9	H		9	9	6	1 Q,S *Bx,Hm
	10	L		10	8	7	2 Q,Ab,B
mottled member	4	H		4	4		Q,Ab,C
	6	L		6	6	1	3 Q,K
pseudosedimentary member	3	H		3	1		2 Q,S
	3	L		3	1		3 Q,S
lithic pumice tuff member	3	H		3	3	3	1 Q,Ab
	3	L		3	3	1	1 Q

Table V. (continued)

	Number of Samples	Alteration Group	X-RAY IDENTIFICATION Zeolites	Quartz	K-feldspar	Plagioclase	clays**	OPTICAL IDENTIFICATION OF SECONDARY MINERALS
Dellenite Flows								
upper member	4	H		4	1	2		Q,C,Cl,B
	5	L		2	3	5	1	K,C,Ox
lower member	2	H		2	1	2		Q,C,Cl,B
	6	L	1	6	2	5		Q,C,Cl,B,Ox
Lithic Pumice Tuff								
	2	H		2	1	2	1	Q,C,S
	2	L		2	1	1	1	
Altered samples not assigned to a map unit								
	24		9	20	12	9	9	Q,C,Cl,K,S

* hand specimen observation

** "clays" include unknown minerals with 7Å or larger d-spacings

altered group of the lower member of the second rhyolites by X-ray techniques. In thin section the groundmass of this group was isotropic. The groundmass of the high altered group sample has a faint birefringence but the grain size is small enough that no minerals could be identified in thin section, but quartz could be identified by X-ray techniques. This indicates that the feldspars were probably the first alteration products of the volcanic glass, and quartz followed shortly thereafter. The difference between high and low altered groups of the other map unit members is the disappearance of quartz, potassium feldspar, plagioclase, and clays in the X-ray size range in highly altered samples, testifying to their probable growth during alteration. Considerable amounts of topaz and some bixbyite and hematite were found in hand specimens of the upper member of the second rhyolites.

The first rhyolites are characterized by quartz under the microscope and by clay minerals using X-ray techniques. The pseudosedimentary member is additionally characterized by microscopic sericite and absence of X-ray feldspars. The mottled member, in general, has no plagioclase in the groundmass. Bixbyite and hematite occur in lithophysae and miarolitic cavities of hand specimens of the spheroidal member.

Under the microscope the dellenite flows are characterized by the presence of calcite, chlorite, biotite, and iron oxides.

The lithic pumice tuff map unit has calcite in the high alteration group.

Many of the samples collected are not assigned to a specific map unit but are included as a group in Table V. Several of these samples are ash fall tuffs and most of them contain heulandite, clinoptilolite, and mordenite.

C. LATTICE PARAMETER OF BIXBYITE

The discovery, by the author, of bixbyite in the district generated interest in that mineral, and led to a chemical and structural examination of that mineral from a number of localities.

Bixbyite, $(Mn,Fe)_2O_3$, was first described in 1897 (Penfield and Foote, 1897) from material collected by Maynard Bixby near Simpson, Utah.

The bixbyite that occurs in volcanic rocks is supposedly formed by pneumatolytic or fumarolic processes (Penfield and Foote, 1897; Mason, 1942; de Villiers and Fleischer, 1943; Mason, 1944; and Frondel, 1970). The author would prefer to use the term "vapor phase crystallization" or as Fries, Schaller, and Glass (1942) stated, the "vapors escaping from the cooling flows" because these terms are more explicit than the terms pneumatolytic or fumarolic.

Fermor (1909) described the mineral species sitaparite in the metamorphosed sedimentary manganese ores at Sitapar in the Chhindwara district, Central Provinces, India. Mason (1942) proved by X-ray powder photographs

that bixbyite and sitaparite were structurally identical. De Villiers (1943) suggested that the name partridgeite be applied to those manganese-iron sesquioxides containing less than 10% Fe_2O_3, sitaparite to the sesquioxides containing between 10% and 30% Fe_2O_3, and bixbyite to the mineral with more than 30% Fe_2O_3. De Villiers and Fleischer (1943) pointed out that all manganese-iron sesquioxides from pure Mn_2O_3 to 59% Fe_2O_3 (the compositional range of the six bixbyite occurrences known at that time) were structurally identical and that the name sitaparite should be dropped. Mason (1944) investigated the phase relationships of the system Fe_2O_3-Mn_2O_3 between 600°C and 1000°C and noted that it was unlikely that bixbyite containing more than 30% Fe_2O_3 (650°C) would be found in the metamorphosed manganese ores and that the bixbyite of fumarolic or pneumatolytic origin had 45% Fe_2O_3 or more (formed above 800°C). Gruner (1943) stated that the lattice parameter increased from 9.35Å in Fe_2O_3 rich bixbyite to 9.42Å in artificial Mn_2O_3. Muan and Somiya (1962) investigated the phase relations of the Fe_2O_3-Mn_2O_3 system between 800°C and 1585°C and noted that d-spacings were not suitable for determining compositions of the Mn_2O_3 solid solution phases (bixbyite). Geller and others (1967) found that α-Mn_2O_3 was actually orthorhombic below 35°C. Geller and Espinosa (1970) showed that small amounts of Cr^{3+} and Ga^{3+} substituting

for Mn^{3+} reduced the lattice parameter of bixbyite while small amounts of Sc^{3+} increased it.

A preliminary comparison of the Stateline bixbyite chemical composition and lattice parameter to those of other bixbyite specimens on hand indicated that the relationship of composition to lattice parameter was not a simple one. Additional specimens of bixbyite from various localities were obtained on an open long-term exchange from the Smithsonian Institution, National Museum of Natural History so that the relationship between composition and lattice parameter might be investigated in more detail.

Smithsonian Specimen Number	Locality	Origin
104814	Postmasburg, South Africa	metamorphic
89105	Sitapar Mn mines Chhindwara, India	metamorphic
104254	Black Range, New Mexico	vapor phase crystallization
118763	San Luis, Potosi, Mexico	vapor phase crystallization
119165	Hayden, Arizona	vapor phase crystallization
C 1636	near Simpson, Utah	vapor phase crystallization

The University of Missouri-Rolla Geology Department museum supplied some bixbyite samples. They were:

Specimen Number	Locality	Origin
R 170	Chihuahua, Mexico	vapor phase crystallization
232 B.1	Littlefield (?), Texas	vapor phase crystallization
n233.7	Postmasburg, South Africa	metamorphic

A Debye-Scherrer camera and Straumanis film loading technique were used to determine the lattice parameters of the various bixbyite powders. An iron tube and a General Electric XRD-1 powder unit were used to generate X-rays, and power settings were 30 kvp, 13 ma. X-ray exposure time varied from two to four hours. A final lattice parameter was obtained by plotting the lattice parameter of each reflection that occurred above $2\theta = 120$ degrees versus the corresponding $\cos^2\theta$ and extrapolating the least square fit of the data to $2\theta = 180$ degrees.

Chemical analyses of the bixbyites were determined by comparison to MnO_2-Fe_2O_3 standards on a General Electric XRD-5 spectrometer with a chromium tube.

The results of the lattice parameter-composition measurements are presented in Figure 10. The obvious features depicted are the general decrease in lattice parameter with increasing manganese content in the natural bixbyites, and the constant lattice parameter with changing composition in the artificial bixbyites. Uncertainty in chemical composition is probably as high as

Figure 10. Lattice parameter vs. composition for various bixbyites

Vertical bar measures uncertainty in the lattice parameter. Compositions known to ± 10% absolute.

o = lattice parameters calculated from Muan and Somiya (1962) on the 440 reflection of samples quenched from 884°C and 800°C. Artificial bixbyites.

• = lattice parameters determined at 23°C by Grant and others (1968). Artificial bixbyites.

1. Smithsonian, 118763, San Luis, Potosi, Mexico

2. Smithsonian, 119165, Hayden, Arizona

3. University of Missouri-Rolla, R170, Chihuahua, Mexico

4. Stateline specimen

5. University of Missouri-Rolla, 232B.1, Littlefield (?), Texas

6. Smithsonian, 104254, Black Range, New Mexico

7. Smithsonian, C1636, near Simpson, Utah

8. Smithsonian, 89105, Sitapar Mn mines, Chhindwara, India

9. University of Missouri-Rolla, n233.7, Postmasburg, South Africa

10. Smithsonian, 104814, Postmasburg, South Africa

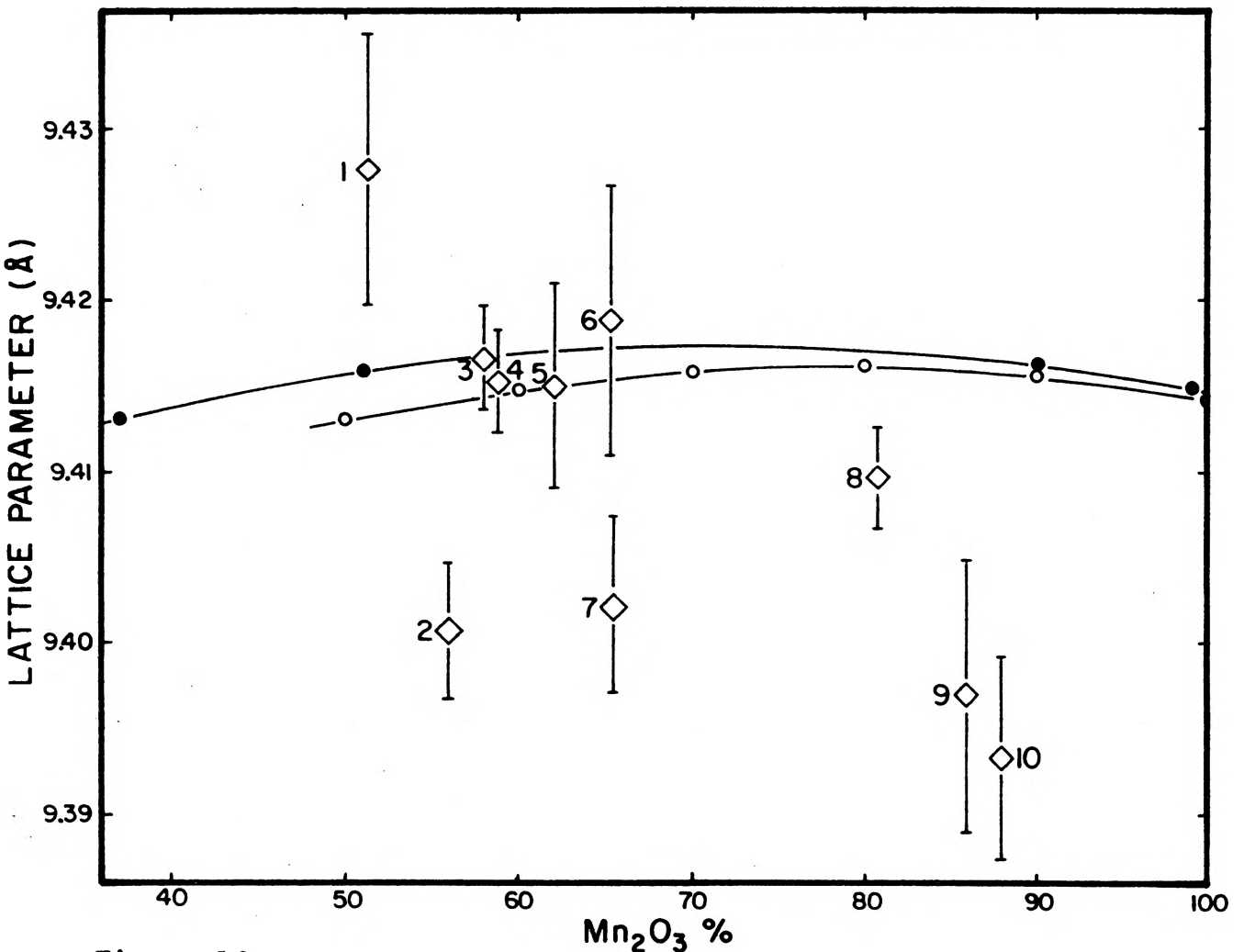
LATTICE PARAMETER (Å)
9.43
9.42
9.41
9.40
9.39
40
50
60
70
80
90
100
Mn_2O_3 %
1
2
3
4
5
6
7
8
9
10

Figure 10.

± 10% (absolute). The lower curve is calculated from the data of Muan and Somiya (1962) where they determined the d-spacing of the 440 reflection of various artificial bixbyites quenched from 884°C and 800°C. The upper curve is controlled by lattice parameters determined at 23°C by Grant and others (1968), on artificial bixbyites of uncertain temperature of formation. Data of Muan and Somiya (1962) indicate that bixbyite quenched at 987°C has the same lattice parameter as bixbyite quenched at 800°C, so temperature of formation probably has little effect on the unit cell dimensions. As previously noted Sc^{3+} increases the lattice parameter of Mn_2O_3, while Cr^{3+} and Ga^{3+} reduce it. Phase relations suggest that high iron bixbyites form at higher temperatures than manganese rich bixbyites. Temperature of formation may affect the partition coefficient of minor elements in a systematic way, leading to the regular variation of parameter with major element composition noted in the natural bixbyites. Also, the concentration of parameter-increasing elements might be higher in a fluid that forms iron rich bixbyites, because of similar chemical properties between those elements and iron. Since the iron rich natural bixbyites have cell dimensions larger than those of the artificial curves of Figure 10, and high manganese bixbyites have smaller parameters, at least two minor elements must vary systematically with the major element composition of the bixbyites. The samples were not tested for their minor

element content, but the Stateline bixbyite (sample 4 of Figure 10) probably has none of these lattice-modifying minor elements, or if present their effects are cancelled. Minor element analysis of the bixbyites is the next logical step to test the hypothesis presented here.

VIII. ALTERATION OF THE VOLCANIC ROCKS

Insights into the nature and degree of alteration in the district are developed through consideration of the map location of altered areas, a division of samples into groups showing low and high alteration, presentation of the chemical analyses in terms of grams oxide per cubic cm of rock to monitor absolute changes, a test of the differences between high and low alteration groups for statistical significance, using differences in variance as an indicator of the style of alteration, and finally presentation of the profile of chemical changes adjacent to a single vein. The locations of samples used in the study are shown in Figure 11.

A. LOCATION AND DEGREE OF ALTERATION

The thin section of each of the samples located in Figure 11 was assigned an alteration index number. This index number reflected the intensity of alteration, including both deuteric and hydrothermal effects. It ranged from zero (no alteration) to five (most intensely altered). Samples with an index number less than three are placed in a low alteration group, for purposes of discussion, while those with an index of three or higher are placed in the high alteration group.

An averaging technique was used to produce the data contoured in Figure 12. A grid overlay with 1½ inch squares was placed over the sample map. An average index

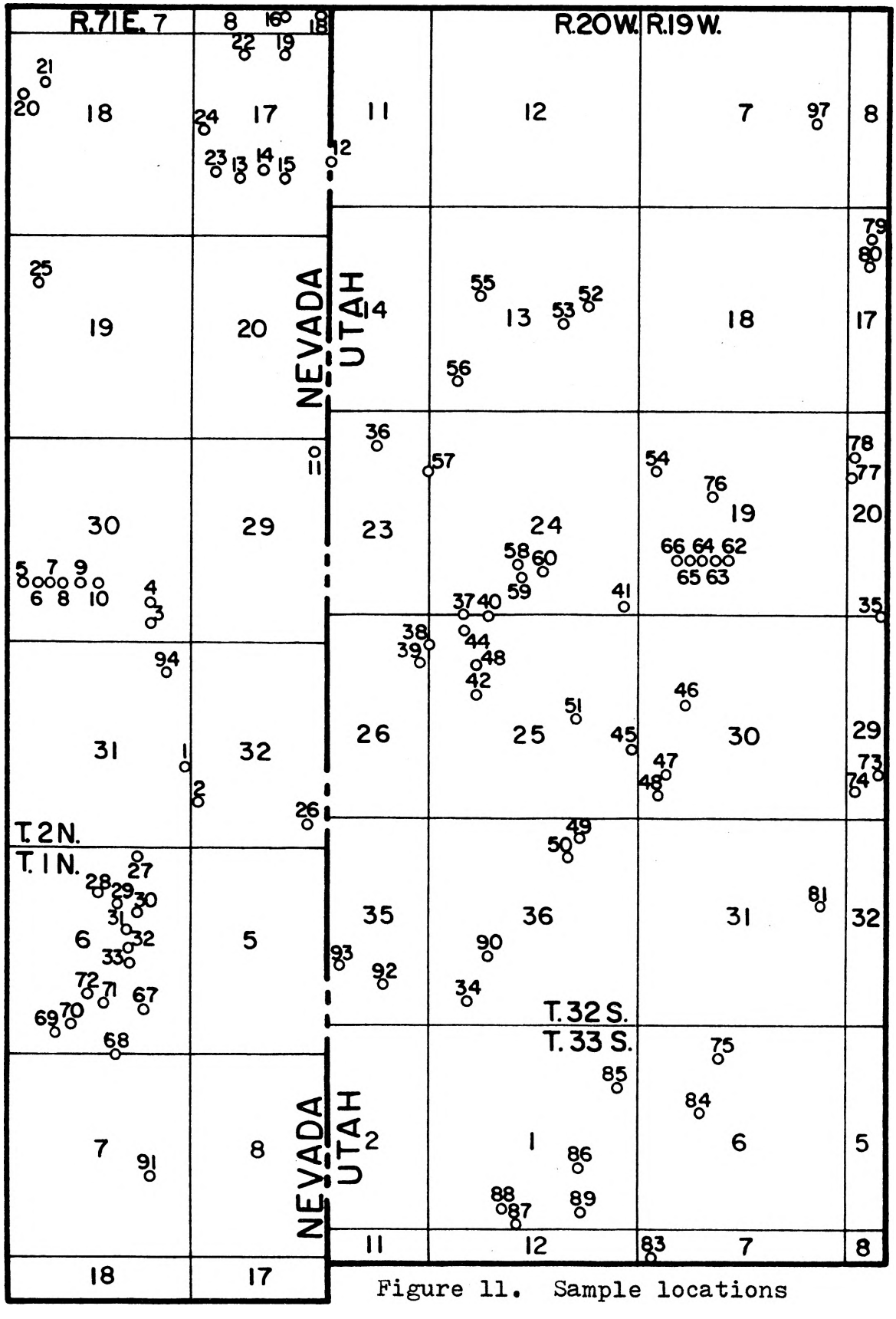

Figure 11. Sample locations

Figure 12. Alteration intensity and vein distribution

Contours of average alteration indices (see text). Dark lines show locations of veins. Area is the same area as in Figure 11.

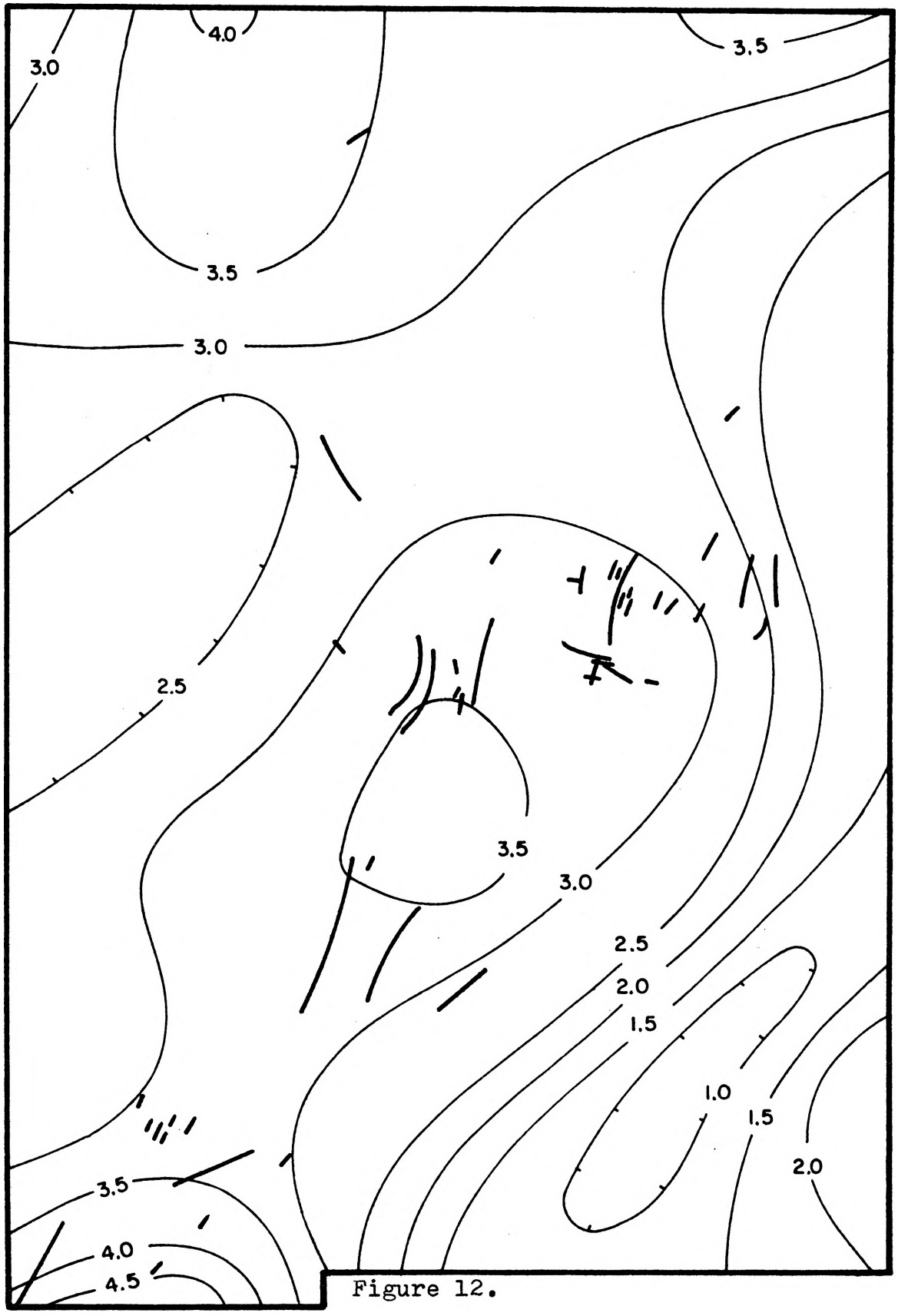

Figure 12.

number at each grid point was obtained using all samples within 1½ inch of the grid point. The grid points were then contoured. This process removed local effects.

The obvious feature depicted by the contoured alteration index map is the arcuate high ridge of alteration that appears at the southwest corner of the map and trends northeasterly to the center of the map and then swings northwesterly through the northwest corner of the map. The veins observed in the field are also plotted on the alteration index map. The veins are coincident with the arcuate ridge of alteration.

B. ALTERATION RESPONSE OF THE STRATIGRAPHIC UNITS

Changes in the map units and members during alteration were monitored by observing chemical changes in the high and low alteration groups. For each group, the decimal concentration of an oxide in each of the samples was multiplied by the sample bulk density to obtain grams oxide/cm^3 of rock, the best quantity with which to measure absolute alteration gains or losses. The bulk density as well as the grain density and porosity of each sample used in this section are tabulated in Appendix B. The difference between the low and high alteration group means, in g/cm^3, for the various members of the map units are detailed in Table VI. The underlined categories are those that showed significant gains or losses with increased alteration. Their significance was established with a two tail t-test

TABLE VI

NET GAINS OR LOSSES DURING ALTERATION

$\bar{x}_H - \bar{x}_L$ is expressed in g/cm^3

	SiO_2	TiO_2	Fe_2O_3	CaO	K_2O
Second Rhyolites					
upper member	-.07	0	.009	-.006	-.024
lower member	.25	-.001	-.006	-.006	-.009
First Rhyolites					
spheroidal member	-.04	.0002	.002	0	.011
mottled member	.13	0	.002	.009	.034
pseudosedimentary member	.05	-.001	-.001	0	.016
lithic pumice tuff member	.08	0	-.011	-.003	.038
Dellenite Flows					
upper member	.04	.006	.042*	.032	.015
lower member	-.07	.013	.040	.005	.012
Lithic Pumice Tuff	-.31	-.003	-.005	.034	-.034

* underlined values are significant at 0.90 level, two tail t-test

at the 0.90 level. The upper member of the dellenite flows had a significant gain in Fe_2O_3 during alteration. The lithic pumice tuff map unit had significant losses of SiO_2, TiO_2, and K_2O accompanied by a significant gain of CaO during alteration. Both the mottled member of the first rhyolites and the upper member of the dellenite flows show apparent gains of all oxides during alteration, and K_2O is apparently added to most of the units. The meaning of the apparent gains or losses that are not proven to be significant will be discussed later when they are related to changes in density and porosity. The second rhyolites are so lightly altered that hydrothermal effects are missing.

An attempt to relate gains and losses of individual oxides to the map position of grouped samples failed to produce clear and consistent patterns. The only oxide whose gains were closely related to the degree of alteration was K_2O. Gains in K_2O were high along the same (NW) to (C) to (SW) trend that also showed a high average alteration index.

Bulk density, grain density, and porosity changes accompany the chemical changes observed during alteration. Table VII indicates the bulk density, grain density, and porosity means of the low and high alteration groups of the members of the map units. The underlined values indicate those categories that are significantly different

TABLE VII

DENSITIES AND POROSITIES, AS AFFECTED BY ALTERATION

	LOW ATLERATION GROUP			HIGH ALTERATION GROUP		
	Bulk Density g/cm^3	Grain Density g/cm^3	Porosity %	Bulk Density g/cm^3	Grain Density g/cm^3	Porosity %
Second Rhyolites						
upper member	2.408	2.587	6.916	2.385	2.582	7.640
lower member	2.353	2.398	1.850	2.478	2.525	1.856
First Rhyolites						
spheroidal member	2.350	2.577	8.825	2.334	2.555	8.602
mottled member	2.374	2.564	7.416	2.536*	2.609	2.791
pseudosedimentary member	2.120	2.605	18.613	2.349	2.649	11.337
lithic pumice tuff member	1.985	2.505	20.956	2.049	2.489	17.762
Dellenite Flows						
upper member	2.430	2.553	4.825	2.513	2.671	5.941
lower member	2.485	2.601	4.198	2.507	2.690	6.801
Lithic Pumice Tuff	2.337	2.570	9.025	2.000	2.539	21.179

* underlined values are significant at the 0.90 level, two tail t-test

between the two alteration groups. They are determined by a two tail t-test at the 0.90 level. The lithic pumice tuff map unit has a significant decrease in bulk density, with increased alteration, while the upper member of the dellenite flows and the pseudosedimentary member of the first rhyolites have significant increases in grain density with increased alteration. The mottled member of the first rhyolites has significant increases of both bulk and grain density accompanied by a significant decrease in porosity.

Density and porosity are related, and changes in density usually coincide with porosity changes. The processes leading to these changes may include leaching (producing cavities) or cavity filling, replacement, and recrystallization or devitrification without an exchange of materials. Leaching that produces cavities should lower the bulk density without affecting grain density, unless the leaching were selective. Porosity would increase. Cavity filling of pore spaces would decrease the porosity, increase the bulk density, and change the grain density, up or down, dependent on the material added to the pore spaces. Replacement without cavity filling or leaching could change the bulk and grain densities without changing the porosity. Devitrification of the glassy fraction could increase the grain density without changing the bulk density. Porosity would increase.

The decrease in porosity of the first rhyolites suggests an active cavity filling process. The lithic pumice tuff map unit was leached, the lower dellenites were devitrified, and the upper dellenites were replaced.

Several relationships can be noted through a comparison of Tables VI and VII. All oxides increased in the mottled member of the first rhyolites during alteration, but in amounts not proven to be significant by individual t-tests. Apparently the significant bulk density, grain density, and porosity changes were in response to the cumulative effect of gains in all oxides, since this would increase the bulk density by filling the pore spaces. In fact, the bulk density did increase and the porosity decreased, so the gains in the oxides, although not proven to be significant, are probably real. The significant increase in grain density of the pseudosedimentary member of the first rhyolites was accompanied by apparent gains of SiO_2 and K_2O. The significant grain density increase in the upper member of the dellenite flows is accompanied by gains of all oxides for which only Fe_2O_3 was significant. The lithic pumice tuff map unit experienced apparent losses of four out of five of the oxides, and at the same time has a significant decrease in bulk density. The porosity is increased, as would be expected, but not by a significant amount.

C. CHARACTER OF THE ALTERATION PROCESS

Alteration has long been classified as being pervasive (homogeneous) or selective (spotty). Deuteric alteration is pervasive on an areal scale but selective in a thin section. Hydrothermal alteration is selective areally but pervasive on a small scale. Pervasive and selective processes should have differing effects on the variance of the major oxides. The rock body being studied would show more oxide variance, among its samples, if the process were areally spotty than if it were pervasive. A pervasive process may even decrease the original variance of the oxides if the process was influenced by the composition of the original rock (selective on a small scale).

Variance of a variable is frequently related to the average value of that variable in the rock body. In fact, a fairly constant ratio (.075) has been observed between variances and means (in oxide percents) for members of the first rhyolites (Figure 13). In this Figure, oxide percents are used instead of g/cm^3 because supporting data are known only in percents. Units cannot be mixed when studying variances or the variance/mean ratios.

The identification of factors that contribute to the total variance and the magnitude of these variations would help to understand the nature of the relationship between the variance and the mean. Variances have the property of being additive, such that the total variance is equal to the sum of the constituent variances. The components of

variation, in this case, can be placed in two broad categories, the lab variations and field variations. The lab variations are those that occur between hand specimens taken from the same outcrop, and include the variances due to both analytical method and sample preparation. The magnitude of the lab variation may be estimated from the dispersion of data points about the powder-slab curves of Figures 7 and 8. The magnitude of the lab factors, expressed as a variance to mean ratio is about 0.03, approximately two-fifths of the total variation.

The analytical variance may be isolated by using ten replicate analyses (page 44) of a single slab, involving five oxides. The analytical variance to mean ratio was less than one-tenth of the total variance to mean ratio.

The field variations are those variations that occur between outcrops within a member and include alteration effects and primary variations. The alteration effect has been illustrated in Figure 13 and is the difference between the high alteration group and low alteration group variances for a particular oxide within a member. It contributes about 0.011 in terms of variance to mean ratios. The "primary" variation (including any other unidentified factors) is the variation that remains after the lab variations are subtracted from the total. The dashed line of Figure 13 is the total variation exclusive of alteration and has a slope of 0.075. The "primary" variation, ratio of variance to mean, is about 0.045.

Figure 13. Variance vs. mean, high and low alteration groups, for members of the first rhyolites, in percent

S = spheroidal member

M = mottled member

P = pseudosedimentary member

L = lithic pumice tuff member

	Alteration Group	
	low	high
SiO_2	o	●
K_2O	□	■
Fe_2O_3	◇	◆
CaO	△	▲
TiO_2	▽	▼

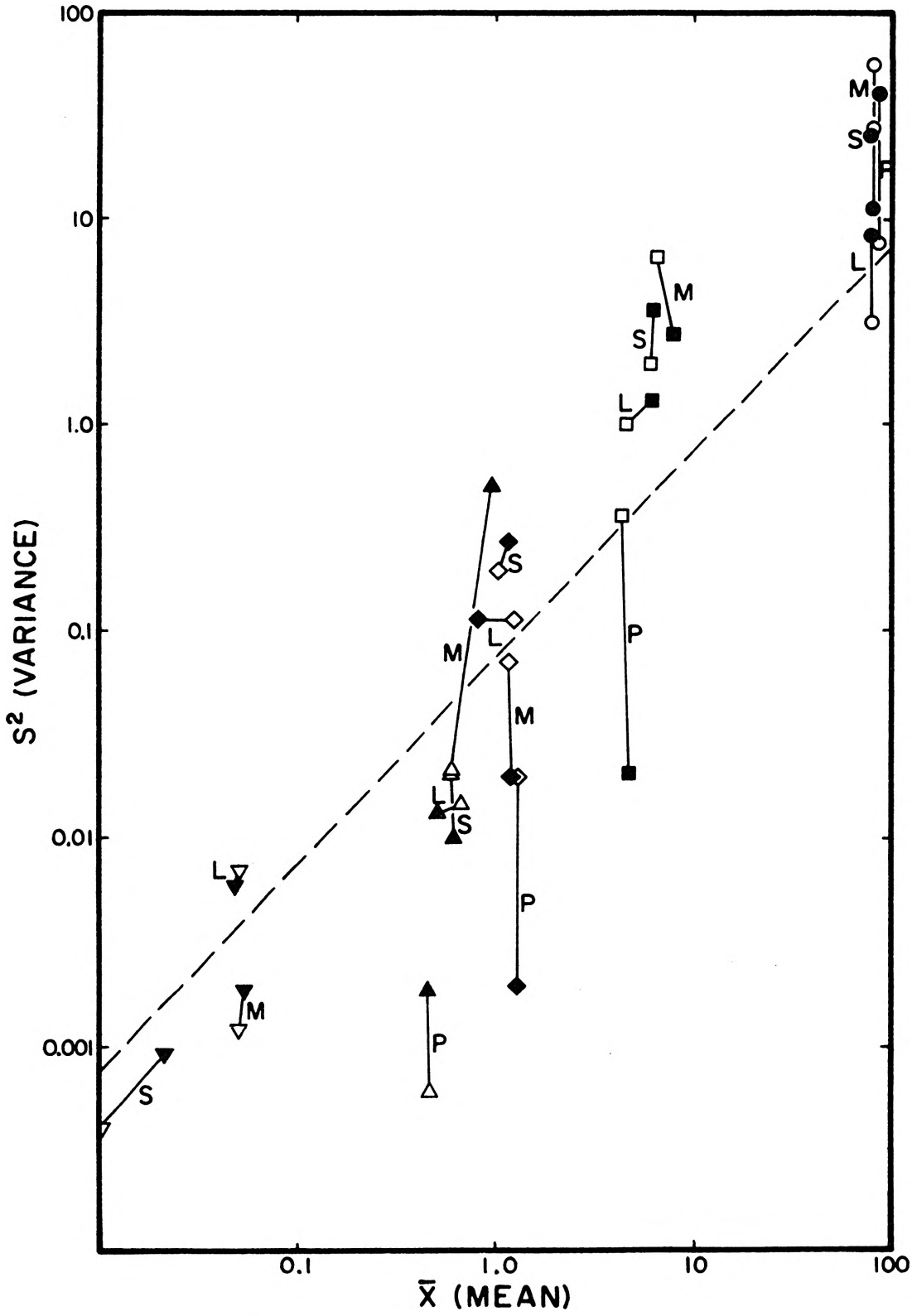

Figure 13.

The reason for the fixed ratio of variance to mean is not known. Binomial data distributions are characterized by a dependence between variance and mean, but this type of distribution has not been generally applied to geologic phenomena (Koch and Link, 1970, p. 205). Assay data (Koch and Link, 1970, p. 299) show a fairly consistent variance to mean ratio, but at a higher level, between one and six, in their case. In the powder-slab data (Figures 7 and 8) the variance increases with the mean.

Figure 13 expresses the sense of alteration and shows that unaltered members are tightly grouped with respect to their means. The open symbols of Figure 13 represent the mean and variance of the low alteration group of individuals in a member and the solid symbols represent the mean and variance of the high alteration group of individuals in the same member. The low alteration groups within a particular oxide plot in a nearly vertical line. This consistency of means suggests that the members of the first rhyolites are related genetically. Members have different variances, dependent on the diversity of the rock types within each.

Alteration appears as large variance shifts and small mean shifts. An increase in variance without a change in the mean shows that the alteration effects are not uniform throughout a member, which indicates that there has been a spotty type of alteration (areally). A decrease

in variance can be attributed to a type of alteration that is more pervasive or "homogenizing" in character. Gains or losses of a particular oxide can be associated with either a spotty or pervasive genesis.

Although many changes are suggested by Figure 13, only a few are significant. These are emphasized in Table VIII for all the altered units. The significance of variance changes during alteration was determined by the F-statistic at the 10% level. Significant increases in variance were noted for TiO_2 in the spheroidal member of the first rhyolites, CaO in the mottled member of the first rhyolites, K_2O in the upper member of the dellenite flows, and Fe_2O_3 in the lithic pumice tuff map unit. Significant decreases were noted for K_2O in the pseudosedimentary member of the first rhyolites and SiO_2 of the lower member of the dellenite flows. It is probably noteworthy that six out of seven members show apparent increases in variance for CaO. Insignificant amounts of CaO were gained or lost within each member so the consistent increase of variances suggests that CaO was probably redistributed within the members during alteration. The sense of this change, to increase the variance, means that the calcium was less homogeneous after alteration than before.

The oxides and lithologies, with the exception of CaO, do not exhibit a clear tendency to follow a selective pattern of increased variance with increased alteration. This seems to indicate that either a pervasive pattern

TABLE VIII

VARIANCE RATIOS, HIGH OVER LOW ALTERATION

	SiO_2	TiO_2	Fe_2O_3	CaO	K_2O
Second Rhyolites	(not significantly altered)				
First Rhyolites					
spheroidal member	0.93	3.42*	1.48	0.53	2.13
mottled member	0.21	1.51	0.34	16.65	0.42
pseudosedimentary member	5.51	∞	0.11	5.95	0.06
lithic pumice tuff member	2.74	0.89	0.96	1.03	1.33
Dellenite Flows					
upper member	0.54	0.68	0.90	3.40	15.36
lower member	0.01	0.92	1.14	4.29	0.15
Lithic Pumice Tuff	0.68	0.25	27.75	8.74	1.62

* underlined values are significant at 0.10 level, F-test

exists or that a weakly developed selective process was active. The likelihood of a weak development, whether pervasive or selective, is supported by subjective comparison of this district with others known to be strongly altered.

If conclusions are to be made from Table VIII, they would include: 1) the cavity-filling process affecting the first rhyolites may have been areally selective (the products of the s_H^2/s_L^2 ratios yield a geometric mean above one), 2) the leaching of the lithic pumice tuff map unit was also selective, 3) the replacement of the upper dellenites was selective, and 4) the devitrification of the lower dellenites was pervasive and must have involved some exchange or redistribution of ions to reduce the variance.

D. ALTERATION ADJACENT TO VEINS

Most of the veins of the district are quartz veins in which lesser amounts of calcite, fluorite, and iron and manganese oxides occur. The veins cut the lithic pumice tuff map unit, dellenite flows, and first rhyolites, but do not cut the second rhyolites. The second rhyolites are noticeably less altered than the underlying map units and are possibly younger than the veins of the district.

Five samples, 72C62 through 72C66, of the mottled member of the first rhyolites were collected along a westward traverse from the quartz-calcite vein located in the SE¼SW¼ sec. 19, T32S, R19W, Utah (EC). Their oxide composition in g/cm^3 was plotted against distance from

the vein, as shown in the lower part of Figure 14. The dashed lines represent the low alteration group means for the various oxides of the mottled member. The upper part of the same figure is a summary, by S.K. Grant, of Tolley (1971), which shows the composite zonation of alteration minerals about several quartz-fluorite veins of the Indian Peak district, located some 15 miles northeast of Stateline, in the Needle Range. Even though the host rocks are different in the two areas, being mainly rhyodacite tuffs and granodiorite at the Indian Peak district, it is interesting to note the similarities in the alteration patterns. In the Stateline area K_2O, SiO_2, Fe_2O_3, and TiO_2 are highest near the vein, while in the Indian Peak area the near-vein minerals are hydromuscovite, quartz, and opaque oxides. Calcium highs in both areas are further from the veins. The distant part of the Stateline profile may be part of an alteration halo about another vein or vein system.

Figure 14. Wallrock alteration profile

Comparison of Stateline vein (see text) with summary of Indian Peak fluorspar district. Dashed lines in the Stateline profile are g/cm^3 means of the low alteration group of the mottled member of the first rhyolites. All samples are from the mottled member.

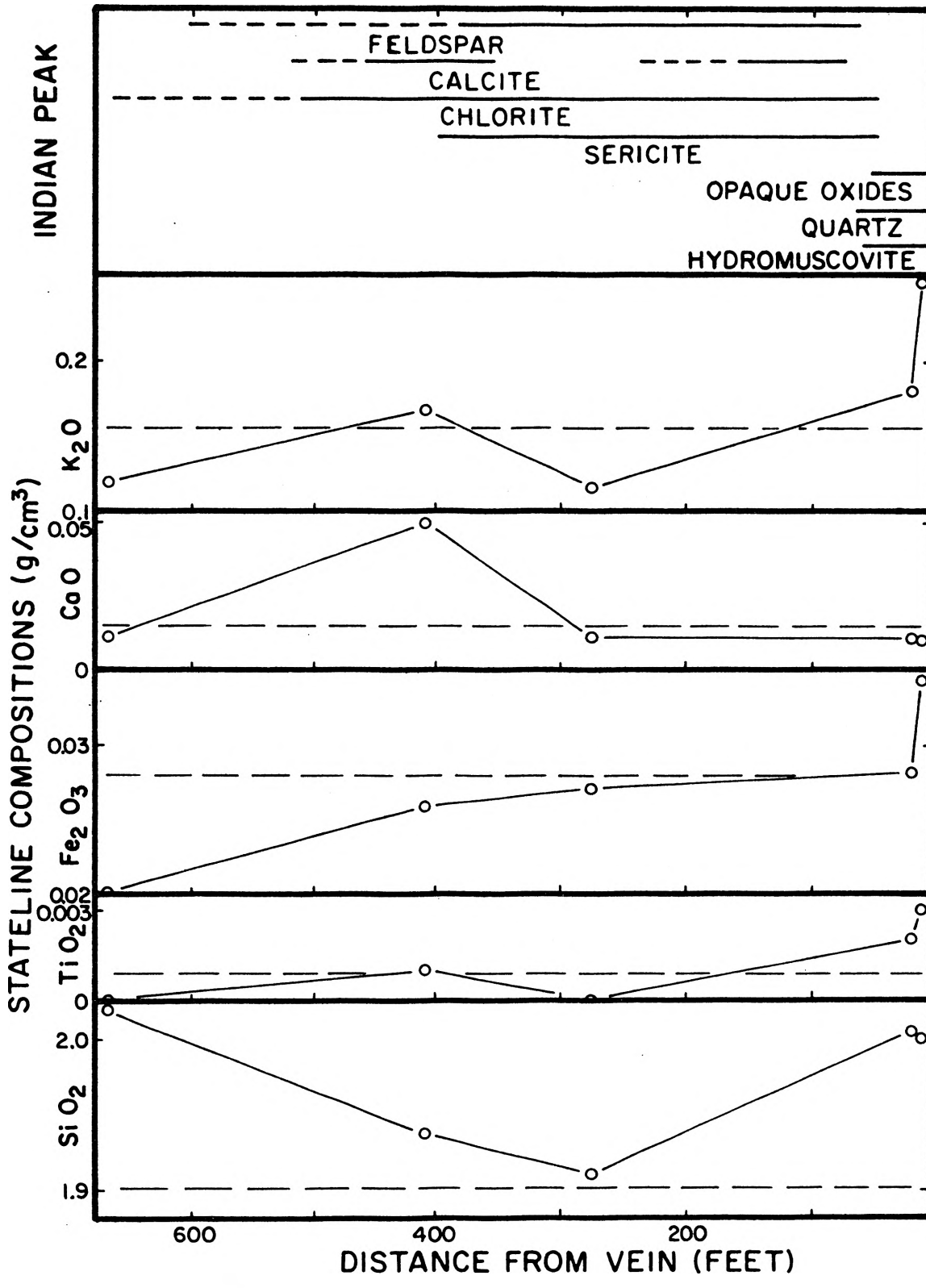
INDIAN PEAK
FELDSPAR
CALCITE
CHLORITE
SERICITE
OPAQUE OXIDES
QUARTZ
HYDROMUSCOVITE
STATELINE COMPOSITIONS (g/cm³)
K2O
0.2
0.1
CaO
0.05
0
Fe2O3
0.03
0.02
TiO2
0.003
0
SiO2
2.0
1.9
600
400
200
DISTANCE FROM VEIN (FEET)

Figure 14.

IX. CONCLUSIONS

The rhyolitic volcanic sequence of the Stateline area is part of the waning stages of a much larger, systematic volcanic cycle that occurred through much of the Tertiary in Western North America. The structures that appear at Stateline are compatible with the tectonic-volcanic framework of the Great Basin, and the rhyolites of Stateline are within an east-west lineament-controlled band of rhyolites that transect the southern Great Basin. The Stateline volcanic stratigraphic section can be recognized in other areas and is probably post-Isom in age.

The four distinct map units recognized are, from oldest to youngest, lithic pumice tuff, dellenite flows, first rhyolites, and second rhyolites. The dellenite flows and second rhyolites are subdivided into lower and upper members, and the first rhyolites are subdivided into the lithic pumice tuff, pseudosedimentary, mottled, and spheroidal members.

The presence of a caldera is suggested by the moat assemblage rocks on the east side of the district, arcuate distribution of veins between Stateline and Gold Springs, and the volcanic doming.

Two general trends of faulting are present, typical north-south Basin and Range type, and an east-west group of faults of varying styles.

Essentially all of the rocks of the district were

determined to be rhyolites or dellenites by X-ray chemical analysis. Map units can be differentiated by chemistry, but members cannot.

Primary mineralogy can also be used to differentiate map units and, when used in conjunction with hand specimen qualities, can be used to distinguish among members.

The secondary minerals of the second rhyolites indicate that this unit is relatively unaltered with respect to the other map units of the district, and also that the first products of the devitrification of volcanic glass are feldspars followed by quartz. Some of the secondary minerals show a preference for certain rock types. The grain size of secondary minerals is dependent on the degree of alteration.

Bixbyite occurs as a secondary mineral associated with topaz and has a lattice parameter of 9.415Å. The parameters of bixbyites from other localities range from 9.393 to 9.428Å, with high-iron varieties having the larger parameters. Since major elements and temperature of formation have been ruled out as direct contributors to the unit cell size, the minor element content may be the determining factor. The minor element content may be influenced by primary element concentration and/or a temperature dependent partition coefficient.

The most intensely altered areas of the district are coincident with the distribution of veins, as are the areas of high K_2O content. Some map units have significant gains

or losses of oxides with increasing alteration. Densities and porosities change during alteration and can be related to chemical gains or losses through processes such as leaching, cavity filling, replacement, or recrystallization without exchange of materials.

The components of the total variance that can be identified and evaluated quantitatively are the lab variations due to analytical method and sample preparation, and the field variations due to primary variations and alteration effects. The variance changes during alteration can be used to classify the character of the alteration process as being either pervasive or selective. When the chemical gains and losses and associated density and porosity changes are considered from this point of view, the leaching, cavity filling, and replacement processes operative in the Stateline area are selective where as devitrification is pervasive.

Chemical variations, including high SiO_2, TiO_2, Fe_2O_3, and K_2O near the vein in the Stateline area are compatible with mineralogical variations that were noted adjacent to veins in other areas.

BIBLIOGRAPHY

Anderson, R. E., Longwell, C. R., Armstrong, R. L., and Marvin, R. F., 1972, Significance of K-Ar ages of Tertiary rocks from the Lake Mead Region, Nevada-Arizona: Geol. Soc. America Bull., v. 83, no. 2, p. 273-288.

Armstrong, R. L. and Higgins, R. E., 1973, K-Ar dating of the beginning of Tertiary volcanism in the Mojave Desert, California: Geol. Soc. America Bull., v. 84, p. 1095-1100.

Atwater, Tanya, 1970, Implications of Plate Tectonics for the Cenozoic Tectonic Evolution of Western North America: Geol. Soc. America Bull., v. 81, no. 12, p. 3513-3536.

Atwater, T., and Molnar, P., 1973, Relative motion of the Pacific and North American plates deduced from sea-floor spreading in the Atlantic, Indian, and south Pacific Oceans: in Kovach, R. L., and Nur, A., editors, Proceedings of the Conference on Tectonic Problems of the San Andreas Fault System: Stanford University Publications Geological Sciences, v. 13, p. 136-148.

Butler, B. S., Loughlin, G. F., Heikes, V. C., and others, 1920, The Ore Deposits of Utah: U.S. Geol. Survey Professional Paper 111, 672 p.

Christiansen, R. L. and Lipman, P. W., 1972, Cenozoic volcanism and plate-tectonic evolution of the Western United States, II Late Cenozoic: Philosophical Transactions, Royal Society of London A. 271, p. 249-284.

Ekren, E. B., Bucknam, R. C., Carr, W. J., Dixon, G. L., and Quinlivan, W. D., 1976, East-trending structural lineaments in central Nevada: U.S. Geol. Survey Professional Paper 986, 16 p.

Elston, W. E., Rhodes, R. C., Coney, P. J., and Deal, E. G., 1976, Progress Report on the Mogollon Plateau volcanic field, southwestern New Mexico, No. 3--Surface expression of a pluton: in Elston, W. E., and Northrop, S. A., editors, Cenozoic Volcanism in southwestern New Mexico: New Mexico Geological Society Special Publication No. 5, p. 3-28.

Elston, W. E., 1976, Tectonic significance of mid-Tertiary volcanism in the Basin and Range province: A critical review with special reference to New Mexico: in Elston, W. E. and Northrop, S. A., editors, Cenozoic volcanism in southwestern New Mexico: New Mexico Geological Society Special Publication No. 5, p. 93-102.

Fermor, L. L., 1909, The manganese-ore deposits of India: Memoir Geological Survey of India, v. 37, p. 49-52.

Fries, Jr., C., Schaller, W. T., and Glass, J. J., 1942, Bixbyite and pseudobrookite from the tin-bearing rhyolite of the Black Range, New Mexico: American Mineralogist, v. 27, p. 305-322.

Frondel, C., 1970, Scandium-rich minerals from rhyolite in the Thomas Range, Utah: American Mineralogist, v. 55, p. 1058-1060.

Geller, S., Cape, J. A., Grant, R. W., and Espinosa, G. P., 1967, Distortion in the crystal structure of α-Mn_2O_3: Physics Letters, v. 24A, no. 7, p. 369-371.

Geller, S., and Espinosa, G. P., 1970, Magnetic and crystallographic transitions in Sc^{3+}, Cr^{3+}, and Ga^{3+} substituted Mn_2O_3: Physical Review B, v. 1, no. 9, p. 3763-3769.

Grant, R. W., Geller, S., Cape, J. A., and Espinosa, G. P., 1968, Magnetic and crystallographic transitions in the α-Mn_2O_3-Fe_2O_3 system: Physical Review, v. 175, no. 2, p. 686-695.

Grant, S. K., Geology and ore deposits of the Indian Peak fluorspar district, Beaver County, Utah: Department of Geology and Geophysics, University of Missouri-Rolla, unpublished manuscript.

Gruner, J. W., 1943, Massive bixbyite $(Mn,Fe)_2O_3$ of low iron content: American Mineralogist, v. 28, p. 174.

Higgins, C. W., 1908, The Jennie and Buck Mountain mines: Salt Lake Mining Review, v. 9, no. 22, p. 15-19.

Koch, Jr., G. S., and Link, R. F., 1970, Statistical analysis of geological data, Vol. I: John Wiley and Sons, Inc., 375 p.

Lawrence, R. D., 1976, Strike-slip faulting terminates the Basin and Range province in Oregon: Geol. Soc. America Bull., v. 87, no. 6, p. 846-850.

Leake, B. E., Hendry, G. L., Kemp A., Plant, A. G., Harrey, P. K., et al, 1969, The chemical analysis of rock powders by automatic X-ray fluorescence: Chemical Geology, v. 5, no. 1, p. 7-86.

Lipman, P. W., 1975, Evolution of the Platoro caldera complex and related volcanic rocks, southeastern San Juan Mountains, Colorado: U.S. Geol. Survey Professional Paper 852, 128 p.

Mason, B., 1942, Bixbyite from Långban. The identity of bixbyite and sitaparite: Geologiska Foreningens Forhandlingar, band 64, haft 2, p. 117-125.

Mason, B., 1944, The system Fe_2O_3-Mn_2O_3: some comments on the names bixbyite, sitaparite, and partridgeite: American Mineralogist, v. 29, p. 66-69.

Muan, A., and Somiya, S., 1962, The system iron oxide-manganese oxide in air: American Journal of Science, v. 260, p. 230-240.

Noble, D. C., Korringa, M. K., Church, S. E., Bowman H. R., Silberman, M. L., and Heropoulos, C. E., 1976, Elemental and isotopic geochemistry of nonhydrated quartz latite glasses from the Eureka Valley Tuff, east-central California: Geol. Soc. America Bull., v. 87, no. 5, p. 754-762.

Nockolds, S. R., 1952, Average chemical compositions of some igneous rocks: Geol. Soc. America Bull., v. 65, no. 10, p. 1007-1032.

Nolan, T. B., 1943, The Basin and Range province in Utah, Nevada, and California: U.S. Geol. Survey Professional Paper 197-D, p. 141-196.

Penfield, S. L., and Foote, H. W., 1897, On bixbyite, a new mineral, and notes on the associated topaz: American Journal of Science, v. 4, p. 105-108.

Rhodes, R. C., 1976, Petrologic framework of the Mogollon Plateau volcanic ring complex, New Mexico--Surface expression of a major batholith: in Elston, W. E., and Northrop, S. A., editors, Cenozoic volcanism in southwestern New Mexico, New Mexico Geological Society Special Publication No. 5, p. 103-112.

Rowley, P. D., and Anderson, J. J., 1975, Guidebook to the Cenozoic structural and volcanic evolution of the southern Marysvale volcanic center, Iron Springs mining district, and adjacent areas, southwestern Utah: Geol. Soc. America Annual Meeting, Field Trip No. 11, 37 p.

Smith, G. H., 1902, Geology of Stateline District: The Mining Review, December 30, Salt Lake City, Utah, p. 67-68.

Smith, G. H., 1902, Stateline Mining District, Iron County, Utah: Mining and Scientific Press, v. 84, no. 8.

Stewart, J. H., Moore, W. J., and Zeitz, I., 1977, East-west patterns of Cenozoic igneous rocks, aeromagnetic anomalies, and mineral deposits, Nevada and Utah: Geol. Soc. America Bull., v. 88, no. 1, p. 67-77.

Thomson, K. C. and Perry, L. I., 1975, Reconnaissance Study of the Stateline Mining District, Iron County, Utah: Utah Geology, v. 2, no. 1, p. 27-47.

Tolley, Michael Allen, 1971, Hydrothermal alteration of ash-flow tuffs in the Indian Peak District of southwestern Utah: M. S. thesis, University of Missouri-Rolla, Rolla, Mo., 87 p.

de Villiers, J. E., 1943, A preliminary description of the new mineral partridgeite: American Mineralogist, v. 28, p. 336-338.

de Villiers, J. E., and Fleischer, M., 1943, A discussion: bixbyite-sitaparite-partridgeite: American Mineralogist, v. 28, p. 468-469.

VITA

Terry Moore Collins was born August 11, 1943 in Long Beach, California. He completed his primary and secondary education in West Plains, Missouri. He was enrolled at the Missouri School of Mines and Metallurgy, Rolla, Missouri, from 1961 through 1963 and attended Lincoln University, Jefferson City, Missouri in 1964. He was first acquainted with geology at Santa Barbara City College, Santa Barbara, California, where he was enrolled from 1965 through the fall of 1966. He returned to the University of Missouri-Rolla for the spring and summer sessions of 1967. The period from 1967 through 1969 was spent in the Army, which included a tour of duty in Viet Nam. He returned to the University of Missouri-Rolla in 1970 and received a B. S. in Geology in the fall of 1971. He and Susan Jane Blickensderfer were married on May 18, 1974.

APPENDIX A

PRIMARY MINERALOGY

	Sample Number	Quartz %	Sanidine %	Plagioclase %	Biotite %	Hornblende %	Total Crystals %	Points counted per thin section
Second Rhyolites								
upper member	72C35	16.7	11.0	10.5	0	0	38.2	621
	73C81	2.0	14.8	7.8	0	0	24.7	594
lower member	72C32	8.2	0	9.0	0.8	0.8	18.8	621
	73C77	11.5	0	15.2	0.7	0	27.3	621
	73C78	6.3	0	7.3	0.2	0	13.8	621
	73C80	7.0	0	15.0	0	0	22.0	594
First Rhyolites								
spheroidal member	72C18	5.0	0.7	0	0.2	0	5.8	594
	72C24	0.3	6.7	0	0	0	7.0	594
	72C26	--	--	--	--	--	--	--
	72C29	5.8	0.8	3.5	1.0	0	11.0	396
	72C31	4.0	3.3	0.5	1.0	0	8.8	396
	72C33	3.5	3.3	2.5	0.2	0	9.5	594
	72C43	4.3	1.0	0	0	0	5.3	396
	72C45	4.3	0	3.0	0	0	7.3	396
	72C47	4.3	1.8	0.5	0	0	6.5	396
	72C49	1.8	3.8	0	0	0	5.5	396
	72C50	7.8	1.3	0	0	0	9.0	396
	72C52	5.0	3.3	1.8	0.3	0	10.3	396
	72C53	4.3	1.3	0.8	0	0	6.3	396
	72C56	6.5	1.8	0	0	0	8.3	396

Appendix A (continued)

	Sample Number	Quartz %	Sanidine %	Plagioclase %	Biotite %	Hornblende %	Total Crystals %	Points counted per thin section
	72C68	0	6.3	0	0	0	6.3	396
	72C69	0.5	11.0	1.0	0	0	11.5	396
	72C72	--	--	--	--	--	--	--
	72C75	0	1.5	1.0	0	0	2.5	396
	73C97	7.5	2.5	0	0	0	10.0	396
mottled member	72C28	5.8	6.0	1.0	0.3	0	13.0	396
	72C30	5.8	3.8	6.5	0.3	0	16.3	396
	72C34	6.2	10.5	0	0.3	0	17.0	594
	72C62	1.3	6.5	0	0	0.3	8.0	396
	72C63	3.5	2.3	0.3	0	0	6.0	396
	72C64	2.8	0.5	0	0.8	0	4.0	396
	72C65	3.5	1.8	0	0	0	5.3	396
	72C66	2.0	6.0	0	0	0	8.0	396
	72C71	4.0	3.3	0.5	0	0	7.8	396
	73C99	0.3	1.8	4.5	0	0	6.5	396
pseudosedimentary member	72C42	3.8	0.3	0.8	0	0	5.0	621
	72C46	5.0	2.5	0	0	0	7.5	396
	72C58	4.3	10.8	0	0	0	15.0	396
	72C59	5.0	9.0	0	0	0	14.0	396
	72C60	5.5	6.3	0	0.3	0	12.0	396
	73C98	4.3	2.0	0	0	0	6.3	396
lithic pumice tuff member	72C14	0.3	1.7	0	0	0	2.0	594

Appendix A (continued)

	Sample Number	Quartz %	Sanidine %	Plagioclase %	Biotite %	Hornblende %	Total Crystals %	Points counted per thin section
	72C48	2.8	3.0	0.5	0	0	6.3	396
	73C83	5.8	7.0	1.5	0	0	14.3	396
	73C85	1.8	0.3	6.0	0	0	8.2	594
	73C87	--	--	--	--	--	--	--
	73C89	1.5	1.3	0	0	0	2.8	594
Dellenite Flows								
upper member	72C02	0	0	24.3	6.2	1.3	31.8	603
	72C04	2.3	0	21.5	6.3	1.5	31.6	594
	72C05	1.7	0	21.8	5.5	0	29.0	621
	72C19	5.0	0	25.3	5.8	0	36.2	621
	72C36	3.2	0	15.2	7.3	0.3	26.0	621
	72C76	0.7	0	22.3	5.7	0	28.7	594
	73C91	0.3	0	15.5	8.0	0	23.8	594
	73C95	0.7	0	19.3	3.2	0.2	23.3	594
	73C96	0	0	24.0	7.2	2.8	34.0	594
lower member	72C12	0	0	14.2	9.7	0.2	24.0	621
	72C15	0	0	12.3	3.7	1.3	17.3	621
	72C16	0.2	0	20.7	5.3	0	26.2	621
	72C22	0	0	26.5	0.5	0	27.0	621
	72C54	0	0	19.0	0.3	0	19.3	621
	72C57	0	0	18.2	3.8	0	22.0	621
	73C92	0	0	16.7	2.5	0	19.2	594
	73C93	0	0	17.2	4.3	0	21.5	594
Lithic Pumice Tuff								
	72C17	2.3	2.0	0.3	0.8	0	5.3	621
	72C20	0.2	0.3	1.5	0.7	0	2.7	621

Appendix A (continued)

	Sample Number	Quartz %	Sanidine %	Plagioclase %	Biotite %	Hornblende %	Total Crystals %	Points counted per thin section
	72C21	3.2	0	4.7	0.2	0	8.0	621
	72C51	4.7	1.5	2.0	0.3	0	8.5	621
Altered slabs, sediments, and ash fall tuffs, etc.								
	72C01	2.5	7.0	0.5	1.0	0	11.0	396
	72C03	16.5	3.5	1.0	2.0	0	23.0	396
	72C06	7.0	6.5	9.5	0	0	23.0	396
	72C07	3.5	3.5	7.5	1.0	0	15.5	396
	72C08	11.3	2.3	6.7	2.0	0	22.3	621
	72C09	10.0	8.3	9.7	2.3	0	30.3	621
	72C10	8.0	6.0	2.5	0.5	0	17.0	396
	72C13	1.3	0	4.0	14.3	0	19.6	621
	72C73	4.3	0	3.0	0.3	0	7.6	621
	73C79	7.0	6.0	7.3	0.3	0	20.6	621
	73C82	1.3	0	15.0	0.3	2.0	18.6	594
	73C94	3.3	1.7	23.7	2.3	0	31.0	594

The following samples were not point-counted because the alteration destroyed the primary mineralogy or, in some cases, because the thin sections were poorly constructed: 72C23, 72C25, 72C27, 72C44, 72C55, 72C67, 72C70, 72C74, 73C84, 73C86, 73C88, 73C90.

APPENDIX B

DENSITY AND POROSITY VALUES

	Sample Number	Bulk Density g/cm^3	Grain Density g/cm^3	Porosity %
HIGH ALTERATION GROUP				
Second Rhyolites				
upper member	73C81	2.385	2.582	7.640
lower member	73C80	2.478	2.525	1.856
First Rhyolites				
spheroidal				
member	72C26	2.140	2.588	16.346
	72C31	2.494	2.584	3.515
	72C33	2.567	2.571	0.157
	72C43	2.522	2.626	3.955
	72C47	2.163	2.561	15.550
	72C53	2.459	2.552	3.633
	72C56	1.990	2.354	15.467
	72C69	2.368	2.576	8.054
	73C97	2.303	2.581	10.739
mottled				
member	72C34	2.551	2.617	2.528
	72C62	2.534	2.613	3.006
	72C63	2.528	2.601	2.804
	72C65	2.532	2.606	2.824
pseudosedimentary				
member	72C42	2.138	2.646	19.202
	72C59	2.473	2.662	7.075
	72C60	2.436	2.640	7.735
lithic pumice tuff				
member	72C14	2.243	2.593	13.510
	72C48	1.988	2.449	18.802
	73C83	1.916	2.425	20.974
Dellenite Flows				
upper member	72C19	2.515	2.697	6.742
	72C36	2.524	2.631	4.085
	73C76	2.387	2.632	9.298
	73C91	2.624	2.723	3.639
lower member	72C12	2.422	2.667	9.181
	73C93	2.592	2.712	4.421
Lithic Pumice Tuff				
	72C20	2.065	2.518	17.966
	72C51	1.934	2.559	24.392

Appendix B (continued)

	Sample Number	Bulk Density g/cm^3	Grain Density g/cm^3	Porosity %
LOW ALTERATION GROUP				
Second Rhyolites				
upper member	72C35	2.408	2.587	6.916
lower member	72C32	2.357	2.394	1.558
	73C77	2.333	2.406	3.018
	73C78	2.370	2.393	0.973
First Rhyolites				
spheroidal member	72C18	2.503	2.574	2.765
	72C24	2.375	2.635	9.857
	72C29	2.477	2.569	3.592
	72C45	2.367	2.546	7.023
	72C49	2.457	2.618	6.174
	72C50	2.434	2.628	7.376
	72C52	2.225	2.572	13.508
	72C68	2.042	2.531	19.330
	72C72	2.516	2.560	1.707
	72C75	2.106	2.535	16.921
mottled member	72C28	2.226	2.496	10.826
	72C30	2.426	2.556	5.092
	72C64	2.365	2.596	8.869
	72C66	2.528	2.569	1.571
	72C71	2.220	2.564	13.392
	73C99	2.479	2.602	4.747
pseudosedimentary member	72C46	2.041	2.584	21.006
	72C58	2.206	2.603	15.252
	73C98	2.113	2.627	19.581
lithic pumice tuff member	73C85	2.307	2.584	10.744
	73C87	1.710	2.394	28.564
	73C89	1.939	2.537	23.561
Dellenite Flows				
upper member	72C02	2.589	2.660	2.652
	72C04	2.474	2.504	1.218
	72C05	2.268	2.564	11.548
	73C95	2.335	2.508	6.904
	73C96	2.483	2.528	1.801

Appendix B (continued)

	Sample Number	Bulk Density g/cm^3	Grain Density g/cm^3	Porosity %
lower member	72C15	2.556	2.604	1.859
	72C16	2.307	2.674	12.203
	72C22	2.615	2.694	2.945
	72C54	2.212	2.331	5.101
	72C57	2.592	2.619	1.030
	73C92	2.628	2.683	2.051
Lithic Pumice Tuff				
	72C17	2.266	2.605	13.003
	72C21	2.407	2.535	5.047

Plate I. Geology of the Stateline District, Utah-Nevada

PLEASE RETURN PLATE TO THE POCKET. COPIES OF THIS PLATE ARE AVAILABLE AT A NOMINAL CHARGE IN THE DEPARTMENTAL OFFICE.

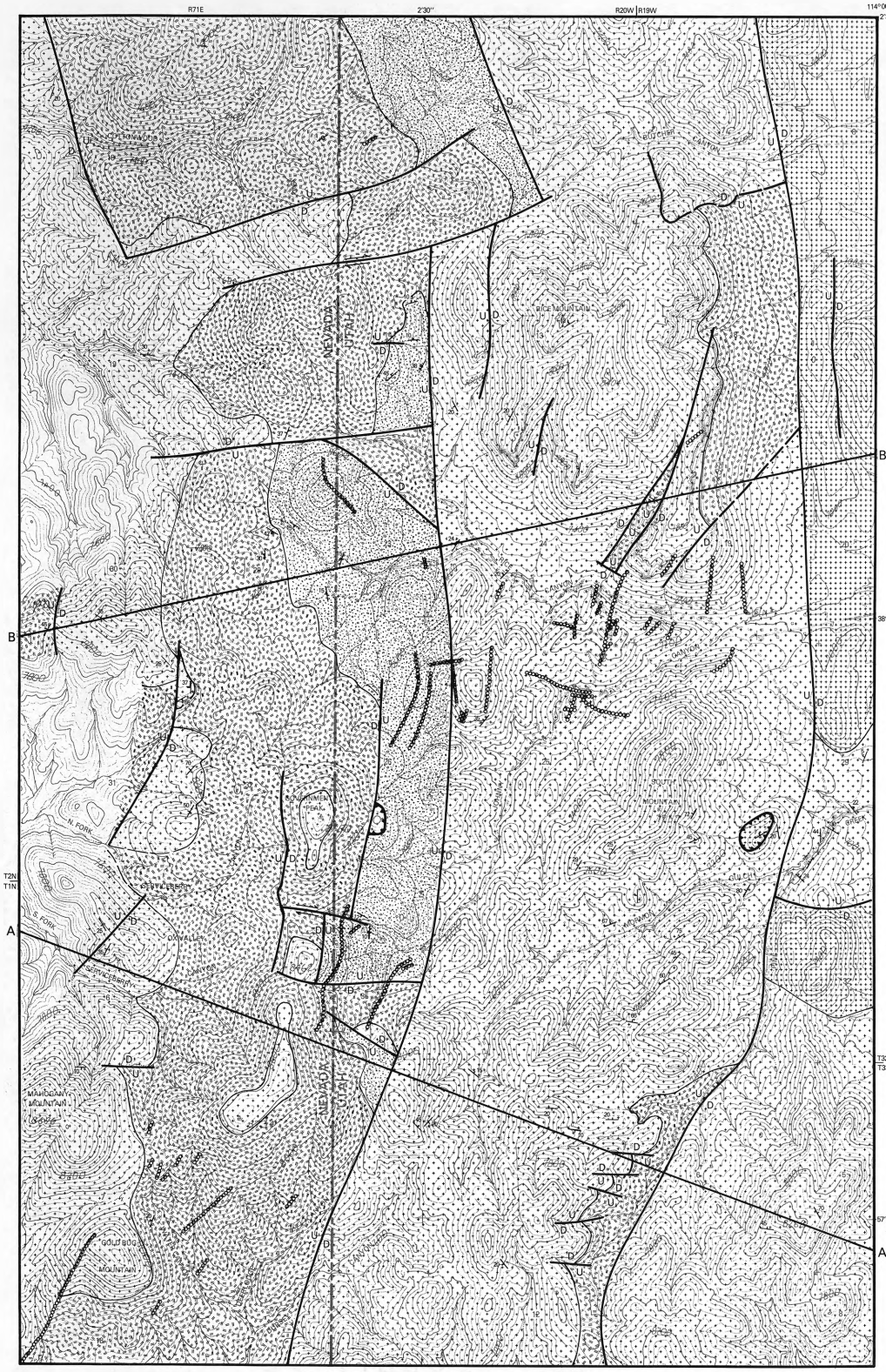

GEOLOGY OF THE STATELINE DISTRICT, UTAH-NEVADA

GEOLOGY BY TERRY M. COLLINS (1972-1973)

SCALE 1:24000

0 1 mile

0 1 kilometer

TN 11°48' GN 32 mils MN 15½° 276 mils

BASE FROM USGS 7½' PRELIMINARY MAPS, LATER NAMED RICE MOUNTAIN AND DEER LODGE CANYON QUADRANGLES

FROM 1977 THESIS BY TERRY M. COLLINS, DEPARTMENT OF GEOLOGY, UNIVERSITY OF MISSOURI - ROLLA

MAGNETIC NORTH (1972)

EXPLANATION

Miocene(?)

- SECOND RHYOLITES
  - Vein
  - Dike
- FIRST RHYOLITES
- DELLENITE FLOWS
- LITHIC PUMICE TUFF

- Contact
- Fault (U / D)
- Low Angle Fault or Slide
- Strike and Dip (15)
- Strike of Vertical Beds

2.5 x VERTICAL EXAGGERATION ON CROSS SECTIONS

- A — A' Line of Section
- Disconformity

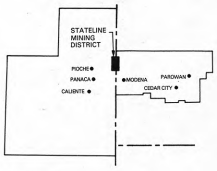

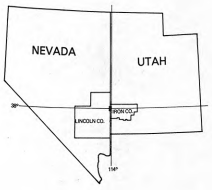

NW	NC	NE
WC	C	EC
SW	SC	SE

DIVISION OF THE MAP AREA INTO REFERENCE SECTORS